深さ 20～30 m の不圧地下水である．上述したように，塩素酸イオンは 2000 μg/L と非常に高濃度で，過塩素酸イオンも 2.6 μg/L と比較的高濃度であった．また，GW1206 と 1608 は，被圧地下水であるが，塩素酸イオン，過塩素酸イオンは比較的高濃度であった．これら地点について，医薬品類[24]や有機フッ素化合物類濃度[28]も測定していたが，本研究では，それらの情報からは，塩素酸イオンや過塩素酸イオン濃度が高かった理由については明らかにはできなかった．

これまで，塩素酸イオン，過塩素酸イオンの起源について，地下水中の医薬品類の存在状況を比較に用いてきた．医薬品類のうち，地下水の下水汚染状況を示すマーカーとして利用されている鎮痒薬のクロタミトン[24]について，両イオンとの関連性について評価した．

図-6 に，本研究の調査対象試料のうち，クロタミトンを測定した試料について，クロタミトンが定量下限値以上の濃度で存在していた場合としていなかった場合の塩素酸イオン濃度と過塩素酸イオン濃度を示す[24]．ノンパラメトリックな検定である，マン・ホイットニーのU検定を用いると，両イオン濃度ともに，クロタミトンが定量下限値以上の濃度で存在した場合としなかった場合で有意差が認められた（$P<0.05$）．すなわち，下水の影響を受けていると考えられる地下水中の塩素酸イオン濃度，過塩素酸イオン濃度は，そうでない場合よりも高い傾向にあることが示された．

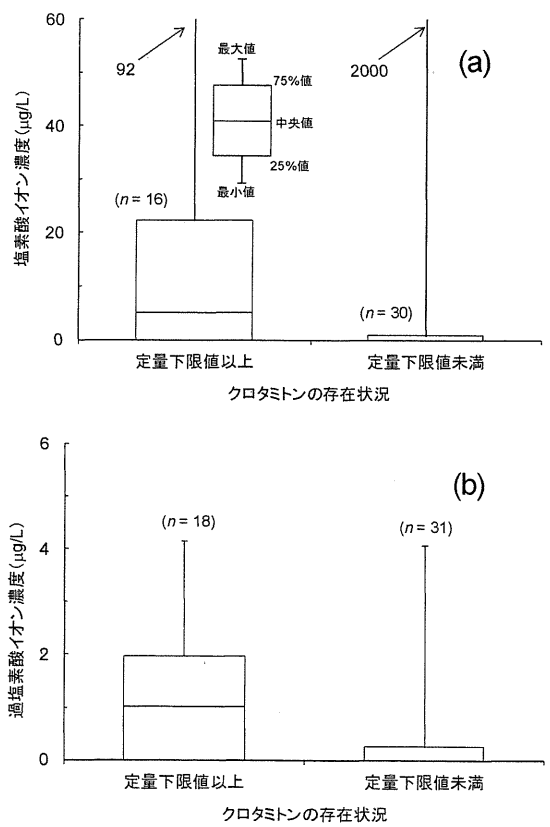

図-6 東京の地下水でクロタミトンが定量下限値以上の濃度で存在していた場合としていなかった場合の (a) 塩素酸イオン濃度および (b) 過塩素酸イオン濃度（定量下限値未満は 0 と表記）[24]

4. まとめ

(1) 本研究で対象とした東京の地下水中の塩素酸イオンは，49試料中24試料が定量下限値以上の濃度で，その範囲は<0.05～2000 μg/L，過塩素酸イオンは，52試料中28試料が定量下限値以上の濃度で，その範囲は<0.01～4.2 μg/Lであった．調査対象試料のうち，25%程度は塩素酸イオンあるいは過塩素酸イオンが比較的高い濃度で存在していた．

(2) 東京の地下水中の塩素酸イオン濃度，過塩素酸イオン濃度を，国内の他の地下水（市販のナチュラルウォーター，専用水道の原水）と比較したところ，東京の地下水中の方が比較的高い濃度の試料が多かったが，定量下限値以上の濃度の試料の割合は最も低く，中央値は同程度であった．

(3) 塩素酸イオン濃度，過塩素酸イオン濃度が比較的高かった試料について，その起源を推定したところ，不圧地下水や湧水の場合，塩素酸イオン濃度が2000 μg/LであったGW1402以外では，水道水や下水による影響を受けている可能性があると考えられた．

謝辞：本研究は，厚生労働科学研究費補助金（H22-健危-一般-006），科学研究費補助金基盤研究（B）22404012およびCREST「都市地下帯水層を利用した高度リスク管理型水再利用システムの構築」によって行われた．記して謝意を表する．

参考文献

1) 厚生労働省健康局水道課：水質基準の見直しにおける検討概要．http://www.mhlw.go.jp/topics/bukyoku/kenkou/suido/kijun/konkyo0303.html
2) 厚生労働省健康局水道課：水質基準省令の改正等について平成 20 年 4 月 1 日施行，2007．http://www.mhlw.go.jp/topics/bukyoku/kenkou/suido/kijun/suishitsu.html
3) 化学工業日報社：2011 年版 15911 の化学商品，化学工業日報社，2011.
4) 化学工業日報社：2004 年版農薬の手引き，化学工業日報社，2004.
5) 厚生労働省健康局水道課：水道水質基準について．http://www.mhlw.go.jp/topics/bukyoku/kenkou/suido/kijun/kijunchi.html

6) Interstate Technology & Regulatory Council (ITRC): Perchlorate Team, Perchlorate: Overview of Issues, Status, and Remedial Options, 2005.
7) The Department of Defense Environmental Data Quality Workgroup: DoD Perchlorate Handbook, 2006.
8) Massachusetts Department of Environmental Protection: The Occurrence and Sources of Perchlorate in Massachusetts (Draft Report), 2005.
9) Kosaka, K., Asami, M. and Kunikane, S.: Perchlorate: origin and occurrence in drinking water, *Encyclopedia of Environmental Health*, Vol. 4, pp. 371–379, 2011.
10) National Research Council: *Health Implications of Perchlorate Ingestion*, National Academies Press, 2005.
11) United States Environmental Protection Agencies: Perchlorate, 2009. http://water.epa.gov/drink/contaminants/unregulated/perchlorate.cfm
12) California Department of Public Health. http://www.cdph.ca.gov/certlic/drinkingwater/pages/Perchlorate.aspx
13) Massachusetts Department of Environmental Protection. http://www.mass.gov/dep/water/drinking/percinfo.htm#stds
14) Brandhuber, P. and Clark, S.: Perchlorate occurrence mapping, American Water Works Association, 2005.
15) Kosaka, K., Asami, M., Matsuoka, Y., Kamoshita, M. and Kunikane, S.: Occurrence of perchlorate in drinking water sources of metropolitan area in Japan, *Water Res.*, Vol. 41, pp. 3474–3482, 2007.
16) 小坂浩司，浅見真理，松岡雪子，鴨志田公洋，国包章一：利根川流域の浄水場における過塩素酸イオンの実態調査，水環境学会誌，Vol. 30，pp. 361–367，2007.
17) Wilkin, R. T., Fine, D. D. and Burnett, N. G.: Perchlorate behavior in a municipal lake following fireworks displays, *Environ. Sci. Technol.*, Vol. 41, pp. 3966–3971, 2007.
18) Rao, B., Hatzinger, P. B., Bohlke, J. K., Sturchio, N. C., Andraski, B. J., Eckardt, F. D. and Jackson, W. A.: Natural chlorate in the environment: Application of a new IC-ESI/MS/MS method with a $Cl^{18}O_3^-$ internal standard, *Environ. Sci. Technol.*, Vol. 44, pp. 8429–8434, 2010.
19) Parker, D. R., Seyfferth, A. L. and Reese, B. K.: Perchlorate in groundwater: A synoptic of "pristine" sites in the coterminous united states, *Environ. Sci. Technol.*, Vol. 42, pp. 146–1471, 2008.
20) 日本水道協会：水道統計水質編（平成 21 年度版），日本水道協会，2011.
21) 国土交通省土地・水資源局水資源部：震災時地下水利用指針（案），2009．http://www.mlit.go.jp/tochimizushigen/mizsei/f_groundwater/shinsaizi.pdf
22) 厚生労働省健康局水道課：流域水質の総合的な保全・改善のための連携方策（緊急時の水質リスクに対応した連携方策）検討調査報告書，2006．http://www.mhlw.go.jp/topics/bukyoku/kenkou/suido/ryuiki/index.html
23) 渡部春奈，村上道夫，小村拓也，諸泉利嗣，古米弘明：国内主要都市における水収支構造と水利用ストレスの評価，用水と廃水，Vol. 51，pp. 137–148，2009.
24) Kuroda, K., Murakami, M., Oguma, K., Muramatsu, Y., Takada, H. and Takizawa, S.: Assessment of groundwater pollution in Tokyo using PPCPs as sewage markers, *Environ. Sci. Technol.*, Vol. 46, pp. 1455–1464, 2012.
25) 厚生労働省健康局水道課：第 7 回厚生科学審議会生活環境水道部会資料，2008．http://www.mhlw.go.jp/topics/bukyoku/kenkou/suido/tantousya/2008/01.html
26) 浅見真理，小坂浩司，吉田伸江，国包章一：水環境，水道水及び次亜塩素酸ナトリウム溶液における塩素酸と過塩素酸の存在状況と相互関係，水道協会雑誌，Vol. 883，pp. 7–22，2008.
27) Weinberg, H. S., Delcomyn, C. A. and Unnam, V.: Bromate in chlorinated drinking waters: Occurrence and implications for future regulation, *Environ. Sci. Technol.*, Vol. 37, pp. 3104–3110, 2003.
28) Snyder, S. A., Vanderford, B. J. and Rexing, D. J.: Trace analysis of bromate, chlorate, iodate, and perchlorate in natural and bottled waters, *Environ. Sci. Technol.*, Vol. 39, pp. 4586–4593, 2005.
29) Murakami, M., Kuroda, K., Sato, N., Fukushi, T., Takizawa, S. and Takada, H.: Groundwater pollution by perfluorinated surfactants in Tokyo, *Environ. Sci. Technol.*, Vol. 43, pp. 3480–3486, 2009.
30) 黒田啓介，福士哲雄，小熊久美子，滝沢智：東京都区部における地下水中の溶存鉄濃度および酸化還元電位の分布特性，日本水文科学会誌，Vol. 38，pp. 63–70，2008.
31) Stetson, S. J., Wanty, R. B., Helsel, D. R., Kalkhoffc, S. J. and Macalady, D. L.: Stability of low levels of perchlorate in drinking water and natural water samples, *Analytica Chimica Acta*, Vol. 567, pp. 108–113, 2006.
32) Asami, M., Kosaka, K. and Yoshida, N.: Occurrence of chlorate and perchlorate in bottled beverages in Japan, *J. Health Sci.*, Vol. 55, pp. 549–553, 2009.
33) Furdui, V. I. and Tomassini, F.: Trends and sources of perchlorate in Arctic snow, *Environ. Sci. Technol.*, Vol. 44, pp. 588–592, 2010.
34) United States Environmental Protection Agencies: Perchlorate Treatment Technology Updates, 2005.
35) Xu, J., Trimble, J. J., Steinberg, L. and Logan, B. E.: Chlorate and nitrate reduction pathways are separately induced in the perchlorate-respiring bacterium *Dechlorosoma* sp. KJ and the chlorate-respiring bacterium *Pseudomonas* sp. PDA, *Water Res.*, Vol. 38, pp. 673–680, 2004.
36) London, M. R., De Long, S. K., Strahota, M. D., Katz, L. E., Speitel, G. E. Jr.: Autohydrogenotropic perchlorate reduction kinetics of a microbial consortium in the presence and absence of nitrate, *Water Res.*, Vol. 45, pp. 6593–6601, 2011.
37) Nakada, N., Kiri, K., Shinohara, H., Harada, A., Kuroda, K., Takizawa, S. and Takada, H.: Evaluation of pharmaceuticals and personal care products as water-soluble molecular markers of sewage, *Environ. Sci. Technol.*, Vol. 42, pp. 6347–6353, 2008.

(2012. 2. 23 受付)

土木学会論文集G(環境), Vol. 69, No. 1, 10-18, 2013.

OCCURRENCE OF CHLORATE AND PERCHLORATE IN GROUNDWATER IN TOKYO

Koji KOSAKA, Keisuke KURODA, Michio MURAKAMI, Nobue YOSHIDA, Mari Asami, Kumiko OGUMA, Satoshi TAKIZAWA and Michihiro AKIBA

Occurrence of chlorate and perchlorate in groundwater in Tokyo was investigated. The samples were collected in 2007 and 2009. Chlorate and perchlorate were detected at the concentrations larger than their determination limits in 24 of 49 and 28 of 52 samples, respectively. Their detection rates in unconfined aquifers and springs were higher than those in confined aquifers. The concentrations of chlorate and perchlorate in about 25% of samples were relatively high, particularly chlorate concentration in one sample (2000 μg/L) exceeded its standard value in drinking water. Compared to other groundwater in Japan (i.e., commercially available natural water and raw water in private water supply), the percentages of the samples with relatively high concentrations of chlorate and perchlorate were higher in groundwater in Tokyo. On the other hand, the percentages of the samples in which chlorate and perchlorate concentrations were larger than determination limits were the lowest. The medians of chlorate and perchlorate in the in groundwater in Tokyo were similar to those in other groundwater in Japan. It was suggested that origins of chlorate and perchlorate in groundwater were drinking water and/or sewage in many cases when their concentrations in groundwater were relatively high.

Separation and Purification Technology 113 (2013) 75–82

Contents lists available at SciVerse ScienceDirect

Separation and Purification Technology

journal homepage: www.elsevier.com/locate/seppur

Natural organic matter that penetrates or does not penetrate activated carbon and competes or does not compete with geosmin

Yoshihiko Matsui [a,*], Soichi Nakao [b], Tomoaki Yoshida [b], Takuma Taniguchi [b], Taku Matsushita [a]

[a] Faculty of Engineering, Hokkaido University, N13W8, Sapporo 060-8628, Japan
[b] Graduate School of Engineering, Hokkaido University, N13W8, Sapporo 060-8628, Japan

ARTICLE INFO

Article history:
Received 11 August 2012
Received in revised form 12 December 2012
Accepted 8 April 2013
Available online 19 April 2013

Keywords:
Super-fine
Submicron
Powdered activated carbon
Natural organic matter
Water treatment

ABSTRACT

The adverse effect of natural organic matter (NOM) on the capacity of activated carbon to adsorb 2-methylisoborneol (MIB), a compound with an earthy/musty odor, is less severe for submicron-sized powdered activated carbon (SPAC) than for conventionally sized powdered activated carbon (PAC) [11]. In this study the NOM effect was confirmed, and the mechanism responsible for the effect was investigated by studies with another malodorous compound, geosmin. The mechanism was investigated with respect to the properties of NOM by simplified equivalent background compound (EBC) estimation and penetration index. Correlations between penetration index values and fractional areas of size-exclusion chromatogram indicated that higher NOM loading on SPAC were associated mainly with a fraction of NOM having a molecular weight (MW) >2 kDa and a chromophoric moiety, which did not diffuse into the inner region of adsorbent particles and instead adsorbed only onto their external surfaces. Therefore SPAC, which has a larger specific surface area per unit mass of adsorbent, adsorbs such high-MW chromophoric NOM to a greater extent than does PAC. However, such NOM does not compete for adsorption sites with geosmin because geosmin adsorbs onto the interior surfaces of adsorbent particles. Contrariwise, NOM with a MW of <2 kDa and with an nonchromophoric moiety penetrates adsorbent particles and adsorbs onto interior surfaces. The estimated EBC concentration and its correlations with both size-exclusion chromatogram fractions and penetration index values indicated the characteristics of the NOM that competes with geosmin to be similar to those of MIB. Chromophoric NOM with a MW of <230 Da competes for adsorption sites with both geosmin and MIB. Beside the nonchromophoric, low-MW (<2 kDa) NOM, such chromophoric, very-low-MW NOM also penetrates adsorbent particles and adsorbs onto interior surfaces. The loading of such NOM is therefore independent of the size of the carbon particles (SPAC or PAC). The NOM effects on geosmin adsorption capacity were therefore found to be similar for SPAC and PAC, despite the fact that more NOM was loaded onto SPAC than PAC. The very-low-MW chromophoric NOM accounted for <2% of the entire NOM.

1. Introduction

Geosmin is a metabolite produced by several classes of microbes, including cyanobacteria and actinomyces, and confers an unpleasant earthy/musty taste and odor to drinking water. Because geosmin has an exceptionally low detention threshold (4 to 10 ng/L) by human taste and smell [1,2], the unpleasant taste and odor can be detected when geosmin is present even in low concentrations, and it can easily affect consumer acceptability. Because drinking water that is aesthetically unacceptable reduces consumer confidence in the water treatment and supply system, the treatment goal for water utilities is to provide drinking water that is not only safe but also acceptable in appearance, taste, and odor.

Adsorption by powdered activated carbon (PAC) is the most conventional treatment method for the removal of micro-pollutants such as geosmin, but the treatment is expensive because of the limited capacity of activated carbon to adsorb geosmin [3]. The presence of natural organic matter (NOM) in untreated water limits the adsorption capacity of activated carbon [4]. NOM is considered to be a target for removal by activated carbon adsorption, but at the same time its loading onto activated carbon reduces the number of adsorption sites available for other compounds, such as geosmin. Because the number of adsorption sites available for adsorptive removal is limited for a given amount of activated carbon, compounds compete for adsorption sites. Because this competition leaves only a few adsorption sites available for compounds present in low concentrations, reducing the concentration of geosmin below its extremely low detention threshold (<10 ng/L) requires large dosages of carbon relative to geosmin concentrations.

* Corresponding author. Tel./fax: +81 11 706 7280.
E-mail address: matsui@eng.hokudai.ac.jp (Y. Matsui).

1383-5866/$ - see front matter © 2013 Elsevier B.V. All rights reserved.
http://dx.doi.org/10.1016/j.seppur.2013.04.009

To improve adsorptive removal efficiency, our research group has proposed the use of submicron-sized super-fine powdered activated carbon (SPAC) [5]. The original concept behind the use of SPAC was to improve the uptake rate of the adsorbate. In fact, adsorptive uptake onto SPAC is very fast, and SPAC is far superior to PAC in removing geosmin and natural organic matter (NOM) in a given contact time [6–8]. Furthermore, the capacity of SPAC to adsorb NOM is higher than that of PAC [5,9]. It has also been reported that the capacity of SPAC and PAC to adsorb 2-methylisoborneol (MIB, another earthy/musty taste and odor compound) decrease to the same extent as a result of NOM loading, although SPAC loads NOM more than PAC [10]. This means that the extra amount of NOM loading on SPAC compared with PAC does not result in an extra reduction of MIB adsorption capacity. The explanation is that the NOM that competes with MIB comprises a small portion of NOM (<2% in dissolved organic carbon, DOC) [11]. It has been reported that the NOM that competes with MIB has a very low MW (<230 Da) and chromophoric properties, and that it adsorbs onto internal pores of activated carbon particles as does MIB, thereby reducing the capacity of activated carbon to adsorb MIB to a similar extent regardless of adsorbent size (SPAC or PAC). The same study has also suggested that the competing NOM has a MW similar to that of the target compound. However, these mechanisms, including the competition between a target compound and the NOM fraction with a similar molecular size, were derived from the results of adsorption experiments with one compound, MIB, in waters containing NOM. Generalization of the mechanisms therefore requires adsorption data for other compounds. Meanwhile, another previous study [9] has suggested that NOM with chromophoric properties is adsorbed onto the external surface of activated carbon particles and is hence adsorbed more on the small particles of SPAC than PAC. These results can be reconciled by hypothesizing that the NOM that adsorbs onto the external surface of activated carbon particles is a high-MW fraction of the chromophoric NOM.

The results of adsorption experiments with various NOMs experimentally verified this hypothesis in the present study. We further investigated the characteristics of the competing NOM and the competition mechanism, which had been reported for MIB, by using another micro-pollutant, geosmin.

2. Materials and methods

2.1. Activated carbon

Commercially available wood-based PAC (Taikou-W, Futamura Chemical Industries Co., Gifu, Japan) was prepared as a slurry in ultrapure water and pulverized to super-fine particles of submicron diameter with a wet bead mill (Metawater Co., Tokyo, Japan). In this paper, we refer to the PAC received directly from the supplier as PAC and the pulverized activated carbon prepared with the wet bead mill as SPAC. The PAC and SPAC were stored as slurries in ultrapure water at 4 °C and used after dilution. Particle size distributions of the activated carbons were determined with a laser-light scattering instrument (LA-700, Horiba, Ltd., Kyoto, Japan) following the addition of a dispersant (0.02 mL of 18% anionic surfactant solution per 200 mL SPAC/PAC sample suspension containing between 0.001% and 0.01% carbon) and a 4-min sonication with ultrasound. Median diameters are 13.5 and 0.86 μm for PAC and SPAC, respectively. BET surface areas were determined with an Autosorb-iQ gas adsorption analyzer (Quantachrome Instruments). BET surface areas are 1070 and 1130 g/m^3 for PAC and SPAC, respectively.

2.2. Water samples

Water samples from Lake Kasumigaura (Ibaraki, Japan) and Lake Hakucho (Hokkaido, Japan) were used as examples of natural waters containing NOM (Table 1S, Supplementary information). After collection and transportation to the laboratory, these samples were filtered through 0.2-μm pore size membrane filters (Hydrophilic PTFE type membrane filter; Toyo Roshi Kaisha, Ltd., Tokyo) and adjusted to a similar DOC concentration of ~1.5 mg-C/L by dilution with ultrapure water (Milli-Q Advantage, Millipore Co.,) amended with salts to obtain a uniform ionic composition. SHA (Suwannee humic acid) waters were prepared by dissolving Suwannee River humic acid in ultrapure water (Milli-Q Advantage, Millipore Co.,) containing inorganic ions added to make the ionic composition similar to that of the Kasumigaura and Hakucho NOM waters.

Stock solutions of geosmin were prepared by dissolving reagent geosmin (Wako Pure Chemical Industries, Ltd., Osaka, Japan) in ultrapure water. Solutions of geosmin in NOM water (NOMW) were prepared by diluting the stock solution of geosmin with the above-described NOMWs to produce geosmin concentrations of about 1 μg/L (5.5 nmol/L). Single-solute solutions of geosmin were prepared by diluting the stock solution of geosmin with organic-free waters (OFWs), which we prepared with ultrapure water containing inorganic ions added to make the ionic composition similar to that of the NOMWs. All waters were filtered through a 0.2-μm pore size membrane filter before use. Geosmin concentrations were analyzed using a Purge and Trap Concentrator Coupled to a GC-MS (GCMS-QP2010 Plus; Shimadzu Corp., Kyoto, Japan; Aqua PT 5000 J, GL Sciences Inc., Tokyo, Japan).

DOC concentrations, measured in sample filtrates with a total organic carbon analyzer (Model 810; Sievers Instruments, Inc., Boulder, CO, USA), served as parameters for bulk NOM quantification. UV absorbance at 260 nm (UV_{260}) was measured with a spectrophotometer (Model UV-240, Shimadzu Corp., Kyoto, Japan) and served as an indicator of chromophoric NOM. The MW distributions of the NOMs were determined by using high performance size exclusion chromatography [HPSEC, HP1100 (Agilent Technologies, Inc., CA, USA); packed column GL-P252 (Hitachi, Ltd.); eluent: 0.02 M Na_2HPO_4 + 0.02 M KH_2PO_4]. Polystyrene sulfonate (weight-average MW 1920, 5180, and 6130 Da) and salicylic acid (138 Da) were used for calibration. The UV_{260} and DOC (Model 810 Turbo; GE Analytical Instruments) of the column effluent were measured continuously.

2.3. Batch adsorption tests

Immediately after addition of a specified amount of SPAC/PAC, the 150-mL vials containing geosmin and/or NOM were shaken and then transferred to a shaker that shook them for one week at a constant temperature of 20 °C. Preliminary experiments confirmed that in one week geosmin adsorption had reached equilibrium and that NOM adsorption equilibrium was almost reached. Control tests were also conducted by using multiple bottles that did not contain carbon to confirm that concentration changes during the long-term mixing were negligible. After the water samples were filtered through a 0.2-μm membrane filter (DISMIC-25HP; Toyo Roshi Kaisha, Ltd., Tokyo), adsorbate (geosmin and NOM) concentrations in the water phase were measured.

3. Results and discussion

3.1. The effect of carbon particle size on geosmin adsorption in the presence of NOM

We conducted geosmin adsorption experiments by using the three NOMWs and the OFW. The capacities of both SPAC and PAC to adsorb geosmin were smaller in all NOMWs than in OFW (Fig. 1S). Ratios of capacities to adsorb geosmin in NOMW vs. OFW at the equilibrium liquid-phase concentration of 100 ng/L

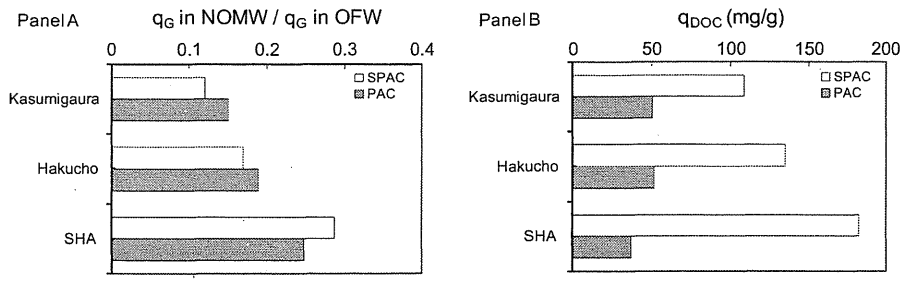

Fig. 1. Panel A: Ratios of geosmin adsorption capacities (designated as "q_G" in the figure) in NOMWs against those in OFW. Panel B: DOC loadings on each carbon. The geosmin adsorption capacities were evaluated by batch adsorption isotherms. Initial and equilibrium geosmin liquid-phase concentrations were 1000 and 100 ng/L, respectively.

are summarized in Fig. 1A. All experiments were conducted at the same initial NOM concentration, but the effects of NOM on geosmin removal were dependent on the type of NOM. The NOM in Kasumigaura water reduced geosmin adsorption to the greatest extent: less than 15% of adsorption capacity remained. However, the amount of DOC in Kasumigaura water that was adsorbed onto carbon was not high compared to the amount of DOC adsorbed from other waters (Fig. 1B). Therefore, the large reduction in geosmin adsorption from Kasumigaura water could not be attributed to the loading of entire NOM. For each of the NOMWs, the ratios of the capacities of SPAC and PAC to adsorb geosmin in NOMW vs. OFW water were similar for SPAC and PAC (Fig. 1A), although SPAC loaded NOM more than PAC (Panel B). This means that the increased amount of NOM loading associated with carbon particle size reduction (from PAC to SPAC) did not result in a further decrease in capacity to adsorb geosmin. Adsorption competition between NOM and geosmin did not become more severe even when NOM loading increased as a result of carbon particle size reduction (from PAC to SPAC).

3.2. Mechanism of NOM competition

The results in Section 3.1 indicate that not all of the NOM competes with geosmin for adsorption sites. Rather, only a portion of NOM seems to be competing with geosmin. Graham et al. [12] estimated the concentration of competing NOM by applying the equivalent background compound (EBC) method and assuming the MW of competing NOM to be 2500 Da: they concluded that the NOM competing with geosmin and MIB was 0.45% of the DOC concentration. The values of EBC parameters, including the initial competing-NOM concentration, are generally determined by a best fit model fit to an experimental isotherm, but the resulting solution for the EBC parameter values is not necessarily unique. In the present study, the amount of competing-NOM loading was estimated by a simplified EBC method, which can avoid the uniqueness problem. When competing NOM is represented by a single hypothetical compound (EBC), the system of micro-pollutant (i.e., geosmin in the present study) in NOMW is modeled as a bi-adsorbate system. The adsorption is described by a Freundlich + IAST (ideal adsorbed solution theory) model.

$$C_G = \frac{q_G}{q_G + q_E}\left(\frac{n_G q_G + n_E q_E}{n_G K_G}\right)^{n_G} \tag{1}$$

where C_G is the liquid-phase concentration of geosmin (nmol/L), q_G is the solid-phase concentration of geosmin (nmol/mg), q_E is the solid-phase concentration of competing NOM (nmol/mg), n_G and K_G are the single-solute Freundlich isotherm exponent and constant, respectively, for geosmin [dimensionless and (nmol/L)/(nmol/mg)$^{1/n}$, respectively], and n_E is the single-solute Freundlich isotherm exponent for EBC (competing NOM) (dimensionless).

With the two assumptions that (i) the solid-phase concentration of the competing NOM is much greater than the solid-phase concentration of the target compound and (ii) the Freundlich exponents of the two adsorbates are not very different, an equation for solid-phase concentration of the competing NOM can be derived [11]:

$$q_E^* \equiv q_E n_E^{\frac{n_G}{n_G-1}} = (n_G K_G)^{\frac{n_G}{n_G-1}}\left(\frac{C_G}{q_C}\right)^{\frac{1}{n_G-1}} \tag{2}$$

where q_E^* is the pseudo solid-phase concentration of competing NOM (nmol/mg).

At high carbon doses in batch adsorption, the mass balances are approximated to;

$$C_{G,0} \cong C_C q_M \tag{3}$$

$$C_{E,0} \cong C_C q_E \tag{4}$$

where $C_{G,0}$ is the initial geosmin concentration (nmol/L); $C_{E,0}$ is the initial concentration of competing NOM (nmol/L).

When carbon doses are high, the isotherm for a micropollutant in natural water can be described by a pseudo-single solute isotherm equation with the same Freundlich exponent as that obtained for the single-solute micropollutant system [13,14]. Therefore,

$$q_G = K_G^* C_G^{\frac{1}{n_G}} \tag{5}$$

where K_G^* is the Freundlich constant describing the geosmin adsorption isotherm obtained in NOMW [(nmol/L)/(nmol/mg)$^{1/n}$].

By substituting Eq. (3) into (5), Eq. (2) becomes;

$$C_{E,0}^* \equiv C_{E,0} n_E^{\frac{n_G}{n_G-1}} = C_{G,0}\left(n_G \frac{K_G}{K_G^*}\right)^{\frac{n_G}{n_G-1}} \tag{6}$$

where $C_{E,0}^*$ is the initial pseudo liquid-phase concentration of competing NOM (nmol/L).

The value of n_E, the EBC Freundlich exponent, was unknown. However, the values of q_E^* and $C_{E,0}^*$ defined by Eqs. (1) and (2), respectively, can be used to compare competing-NOM loadings on the carbon particles and to compare initial competing-NOM concentrations if the n_E values are not very different [11,15].

The fact that values of q_E^* were similar for SPAC and PAC for all tested waters (Fig. 2A) clearly indicates that SPAC and PAC adsorbed competing NOM to similar extents at a given carbon dose. However, SPAC adsorbed NOM to a greater extent at a given carbon dose than PAC did, as shown in Fig. 1B. These results suggest that SPAC adsorbed non-competing NOM (NOM that is not competing with geosmin) to a greater extent than PAC did, but that SPAC and PAC adsorbed competing NOM to similar extents. Accordingly, the magnitudes of the effects of NOM on geosmin adsorption were almost the same for SPAC and PAC. The initial concentrations of the

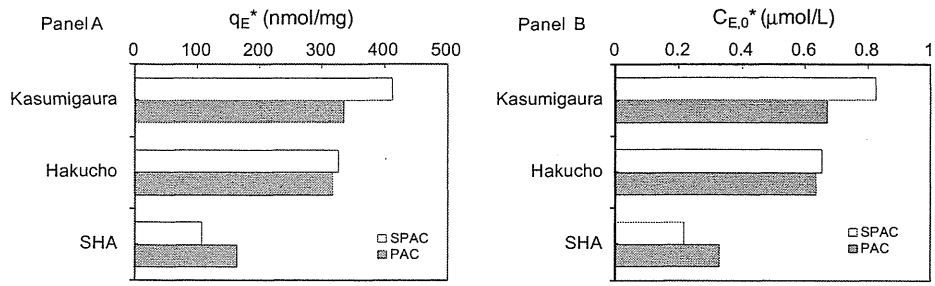

Fig. 2. Panel A: Pseudo solid-phase concentration of geosmin-competing NOM (q_E^*) at a carbon dose of 2 mg/L. Panel B: Initial pseudo liquid-phase concentration of the geosmin-competing NOM ($C_{E,0}^*$).

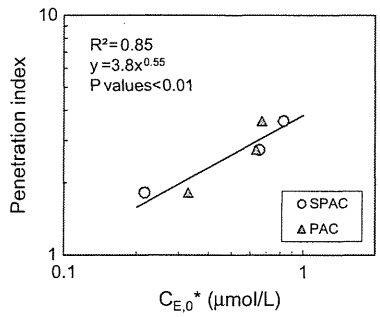

Fig. 3. Relationship between penetration index values and initial pseudo liquid-phase competing-NOM concentrations ($C_{E,0}^*$). The penetration index values were equated to the slope of the logarithm of the median diameter of adsorbent against the logarithm of the DOC solid-phase concentration.

NOM that competes with geosmin ($C_{E,0}^*$) were similar for SPAC and PAC (Fig. 2B).

For MIB adsorption in NOMWs, the values of $C_{E,0}^*$ are highly correlated with the values of the penetration index, which is defined by the slope of plots of the logarithms of the median adsorbent diameters vs. the logarithms of the solid-phase NOM concentrations, and by which the extent of penetration of NOM into carbon particles can be quantitatively evaluated [11,17]. For geosmin in the present study, the correlation obtained was fairly good, as shown in Fig. 3. The positive slope of the correlation plot indicates that the NOM consisted of a high percentage of competing-NOM molecules with a tendency to be highly penetrative. This suggests that the competing NOM penetrated and adsorbed onto interior surfaces of the carbon particles. If so, the extent of competing-NOM loading on SPAC and PAC would be similar. This conclusion is consistent with the results in Fig. 2 and related discussion, in which pseudo solid-phase concentrations, namely, competing-NOM loadings (q_E^*) on SPAC and PAC, were not different.

3.3. Characteristics of NOMs that penetrate and do not penetrate activated carbon

In the previous study of Ando et al. [9], adsorption isotherms on SPAC and PAC were compared for NOM from different sources. These investigators reported that for high-SUVA (specific UV absorbance) NOM the ratio of SPAC to PAC adsorption capacities was high, suggesting that such NOM did not penetrate the carbon particle and preferentially adsorbed near the outer surface of the carbon particle. Instead of this ratio, in the present study we used the reciprocal value of the penetration index, the non-penetration index, to more precisely quantify the degree of limited penetration of NOM from the outer surface to the inner region of carbon particles. We evaluated NOM characteristics by using the data of HPSEC with UV_{260} and DOC detection. We also used NOM adsorption and HPSEC data from previous studies [9,11]. The fact that SUVA values were significantly correlated with non-penetration index values ($R^2 = 0.71$, $P < 0.0001$, Fig. 4A) reflects the tendency of the adsorption capacity to be higher for SPAC than for PAC when the NOM consists mostly of chromophoric NOM. The correlation was much lower but nevertheless significant ($R^2 = 0.28$, $P = 0.028$) between the weight-average MW of the DOC and non-penetration index (Fig. 4B), whereas the correlation was higher and very significant between the weight-average MW of UV_{260} and non-penetration index ($R^2 = 0.75$, $P < 0.0001$, Fig. 4C). These results suggest that MW also plays an important role in the degree of penetration. We then hypothesized that a high-MW fraction of the NOM could penetrate the carbon particle to a lesser extent than a low-MW fraction and would hence preferentially adsorb near the outer surface of activated carbon particles. We calculated the percentages of high-MW NOM fractions in the DOC by integrating partial areas of DOC chromatograms for MWs exceeding certain cutoff levels. We used the product of the SUVA value and the partial area of the UV_{260} chromatograms for MWs exceeding certain cutoff levels as a metric of the chromophoric high-MW fraction. Fig. 5 shows the

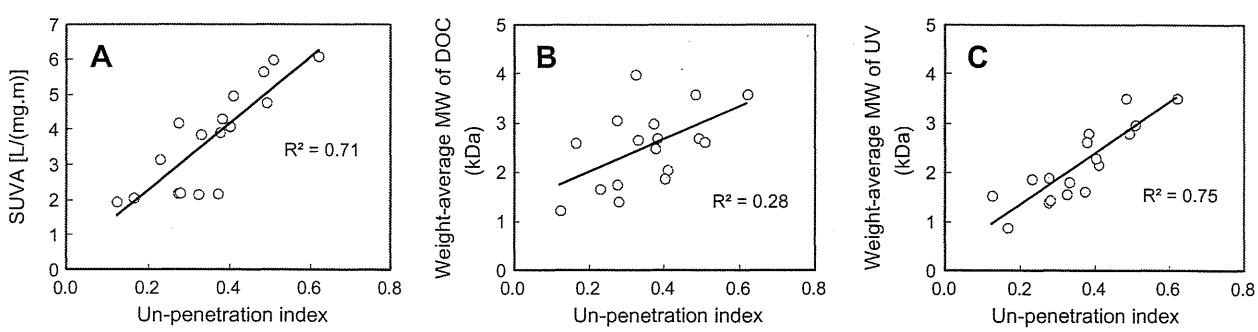

Fig. 4. Plots of un-penetration index values vs. SUVA values (A), weight-average MWs of DOC (B), and weight-average MWs of UV_{260} (C).

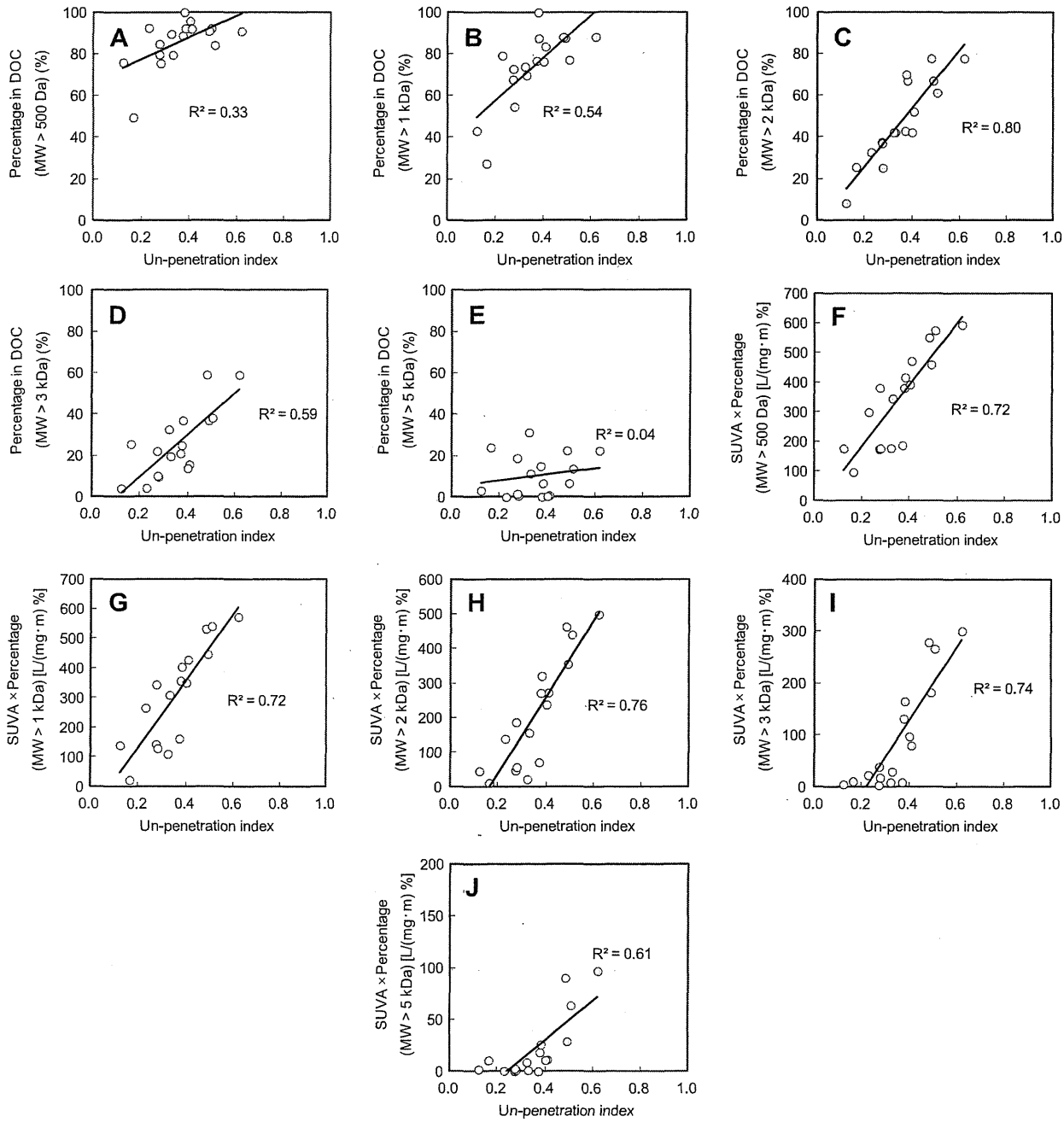

Fig. 5. Plots of un-penetration index values against the fractional areas of DOC chromatograms with MW higher than cutoff levels (Panels A–E) and against the product of SUVA value and fractional areas of UV_{260} chromatogram with MW higher than cutoff levels (Panel F–J).

relationships between the percentages of various high-MW NOM fractions and the non-penetration index values. The correlation was highly significant ($R^2 > 0.7$, $P < 0.0001$) for DOC with MWs of >2 kDa (Fig. 5C) and chromophoric NOM with MWs of >0.5, >1, >2, and > 3 kDa (Fig. 5F–I). Overall, correlations were higher for chromophoric NOM fractions than for DOC fractions (Fig. 6), but a high correlation ($R^2 > 0.75$) was commonly seen for MWs of > 2 kDa for both DOC and chromophoric NOM. It is therefore possible that chromophoric high-MW (MW > 2 kDa) NOM is associated with low penetration into carbon particles. To explore the contrasting characteristics of NOM with high penetrative ability, we plotted low-MW NOM fractional areas, against penetration

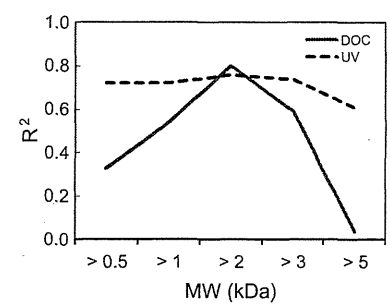

Fig. 6. Change of R^2 for un-penetration index against MW cutoff level.

index values (Fig. 7). A fairly high and significant correlation ($R^2 = 0.69$, $P < 0.0001$) was evident for NOM fractions that consisted of DOC with MWs of <2 kDa (Fig. 7C), but the correlation with chromophoric NOM with MWs of <2 kDa was low and not significant ($P = 0.35$, Fig. 7H, Fig. 8). Therefore nonchromophoric low-MW NOM could probably diffuse into the inner region of carbon particles and adsorb there.

To further confirm these estimates, we divided NOM into four fractions and conducted multiple regression analyses with non-penetration or penetration index values as the dependent variable and the percentages of three NOM fractions out of the total of four fractions as the explanatory (independent) variables. We used a MW of 2 kDa as a cutoff level for the NOM fractionation, on the basis of the results mentioned above in this subsection. The four NOM fractions were (a) chromophoric NOM with MWs of <2 kDa, (b) chromophoric NOM with MWs of >2 kDa, (c) nonchromophoric NOM with MWs of <2 kDa, and (d) nonchromophoric NOM with MWs of >2 kDa (see Table 1). The percentages of the four fractions were calculated from the DOC and UV chromatograms on the basis of the assumption that the SUVA of chromophoric NOM was 6.1 m^{-1} L/mg-C [11,16]. When the non-penetration index was the dependent variable, the explanatory variables were fractions a, b,

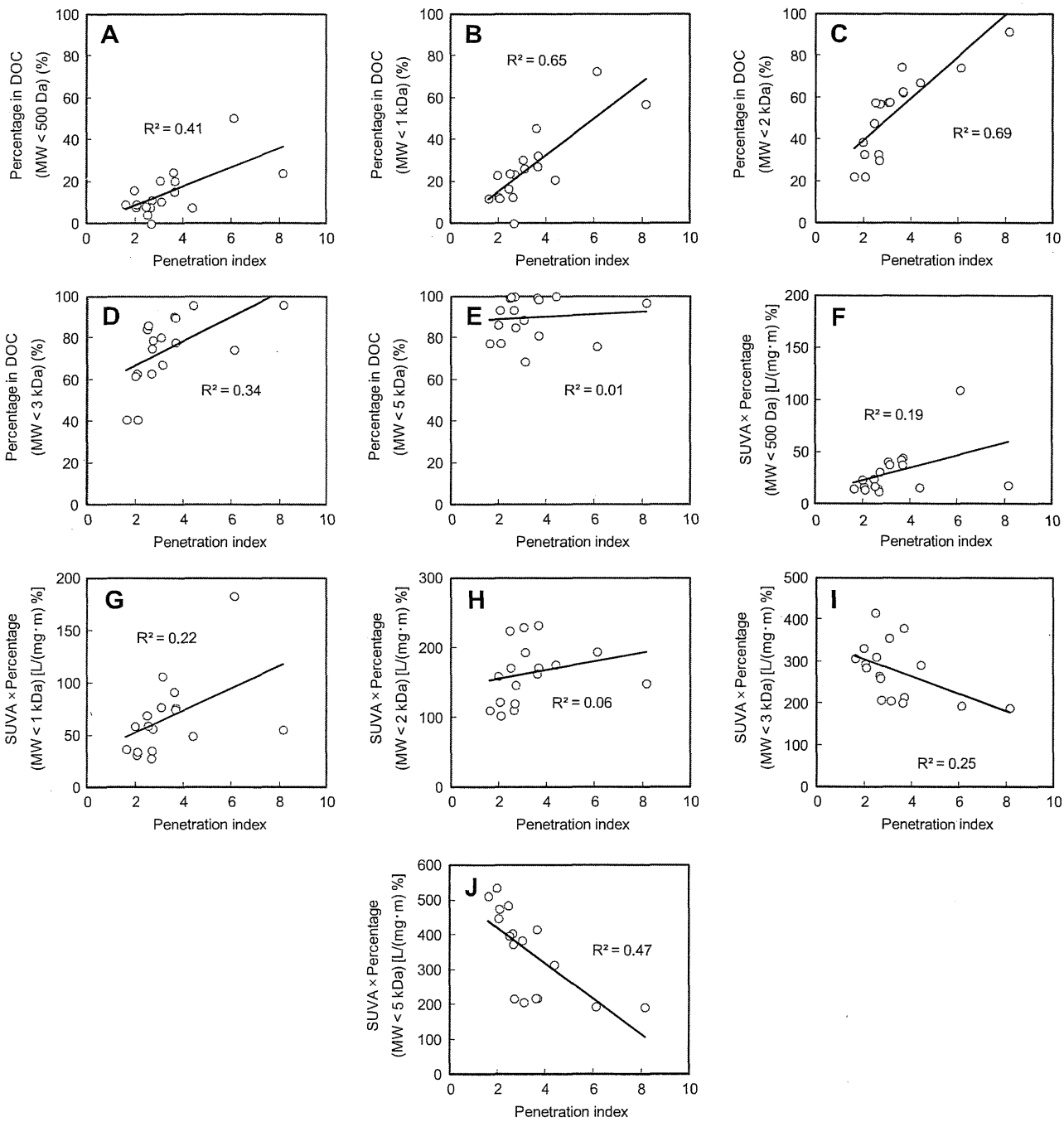

Fig. 7. Plots of penetration index values against the fractional areas of DOC chromatogram with MW lower than cutoff levels (Panels A–E) and against the product of SUVA value and fractional areas of UV_{260} chromatograms with MW lower than cutoff levels (Panels F–J).

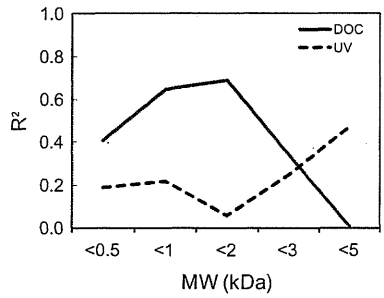

Fig. 8. Change of R^2 for penetration index against MW cutoff level.

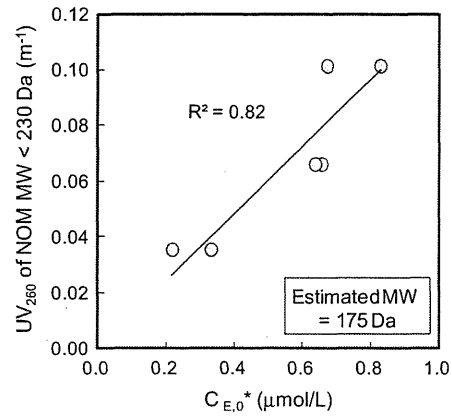

Fig. 9. Relationship between the UV_{260} absorbance of NOM with a MW of <230 Da and the competing-NOM concentration ($C^*_{E,0}$). UV_{260} absorbance values were obtained from size-exclusion chromatograms. $C^*_{E,0}$ values were estimated from geosmin isotherms by using Eq. (2). Coefficients of determination (R^2) were determined from 1 – SSreg/SStot, where SSreg is the sum of squares of the residuals around the regression line with an intercept of 0, and SStot is the sum of squares of the residuals around a horizontal line representing the mean absorbance value of the data shown [18].

and d, fraction c being the most likely to not include non-penetrating NOM. Results are shown in Table 1. Fraction b was associated with a highly significant ($P = 2.2 \times 10^{-5}$) positive regression coefficient. Fraction d was also associated with a significant ($P = 0.028$) positive regression coefficient. It is therefore possible that the NOM that does not penetrate carbon particles and instead adsorbs onto the outer surface of the particles is composed mainly of chromophoric NOM with MWs of >2 kDa. Nonchromophoric NOM with MWs of >2 kDa could also be non-penetrating NOM. When the penetration index was the dependent variable, the explanatory variables were the three fractions a, c, and d, fraction b being the most likely to not include penetrating NOM. The fact that fraction c was associated with a positive and highly significant ($P = 2.8 \times 10^{-5}$) regression coefficient indicates that the penetrating NOM was composed mainly of nonchromophoric NOM with MWs of <2 kDa.

3.4. Characteristics of NOMs that compete and do not compete with geosmin

The previous study [11] revealed that MIB competes with very-low-MW (MW < 230 Da) chromophoric NOM. We assumed the NOM that competes with geosmin to be similar to that of MIB because the MW of geosmin (182 Da) is similar to that of MIB (168 Da). We plotted the UV_{260} absorbance of very-low-MW NOM, which we obtained from the fraction of the area of the UV_{260} chromatogram with MW of <230 Da, against the initial concentration of the NOM that competes with geosmin (Fig. 9). The slope of the linear relationship is the ratio of UV_{260} to $C^*_{E,0}$. The ratio is theoretically given by

$$\frac{UV_{260}}{C^*_{E,0}} = \frac{SUVA \times Cabon\ content \times MW}{n_E^{\frac{n_M}{n_M-1}}} \quad (7)$$

If the NOM that competes with geosmin is a chromophoric NOM, as is the case with MIB, its MW can be estimated by using Eq. (7). The estimated MW was 175 Da if we assumed the SUVA value and carbon content of the chromophoric NOM in Eq. (7) to be 6.12 cm^{-1} L/mg and 52%, respectively (International Humic Substances Society, 2012; [11,16]). The estimated MW of 175 Da corroborated the cutoff MW value of 230 Da. When the cutoff MW values were changed, the estimated MWs changed accordingly, as shown in Table 2. The cutoff MW and the estimated MW were in agreement only when the cutoff MW was 230 Da. When DOC concentrations were used instead of UV_{260} absorbances and the DOC MW fractions were plotted against $C^*_{E,0}$, none of the plots produced agreement between the cutoff and estimated MWs (Table 2). The estimated MW (175 Da) of competing NOM is very close to the MW of geosmin (182 Da). Moreover the R^2 value is also high. The result therefore confirms that the competing NOM has a molecular size similar to that of the targeted micro-pollutant, a conclusion suggested from the MIB experiments [11]. If the MW of the competing NOM is 175 Da, the concentration of competing NOM in the NOM waters accounts for <2% of the total DOC concentration.

Section 3.4 has revealed that the competing NOM consists of very-low-MW (<230 Da) chromophoric NOM, whereas Section 3.2 revealed the competing NOM to be a penetrating-NOM. Therefore, the very-low-MW (<230 Da) chromophoric NOM appears to be a penetrating NOM, though penetrating NOM is composed mainly of low-MW nonchromophoric NOM (Section 3.3). The low-MW nonchromophoric NOM would probably not compete with geosmin, although it diffuses into the inner region and adsorb to internal adsorption sites. Such NOM, because of its molecular size, would not mostly have access to pores where geosmin adsorbs. We also suspect that the adsorption affinity of such NOMs to

Table 1
Regression analyses for NOM that penetrates and does not penetrate activated carbon.

Designation		Fraction a	Fraction b	Fraction c	Fraction d
Dependent variable = un-penetration index value	R^2	Chromophoric NOM		Nonchromophoric NOM	
		MW < 2 kDa	MW > 2 kDa	MW < 2 kDa	MW > 2 kDa
		Fraction a	Fraction b	Fraction c	Fraction d
Coefficient	0.83	0.0014	0.0057		0.0038
P-value		0.60	2.2×10^{-5}		0.028
Dependent variable = penetration index value	R^2	Chromophoric NOM		Nonchromophoric NOM	
		MW < 2 kDa	MW > 2 kDa	MW < 2 kDa	MW > 2 kDa
Coefficient	0.77	0.077		0.085	−0.01
P-value		0.82		2.8×10^{-5}	0.56

Table 2
MW estimated from the slope of the plot of the concentration of the low-MW fraction and competing-NOM concentration, and the coefficients of determination (R^2) of the plots. Coefficients of determination were equated to 1 – SSreg/SStot, where SSreg is the sum of squares of the residuals around the regression line with an intercept of 0, and SStot is the sum of squares of the residuals around a horizontal line representing the mean absorbance value of the data shown [18].

	Cutoff MW (Da)	<1000	<500	<300	<250	<230	<200
UV_{260}	Estimated MW from the slope (Da)	2130	1150	433	263	175	13
	R^2	0.68	0.92	0.73	0.57	0.82	0.29
DOC	Estimated MW from the slope (Da)	5280	3480	2700	2030	1600	1060
	R^2	0.88	0.76	−0.2	−0.41	−4.6	−4.2

activated carbon is weak and hence that they would not compete effectively with a strong adsorbate such as geosmin.

4. Conclusions

NOM with a high-MW (>2 kDa) and with a chromophoric moiety adsorbs onto the external surface of activated carbon particles. Therefore, when NOM consists mostly of such NOM, SPAC adsorbs NOM to a greater extent than does PAC. Contrariwise, low-MW (<2 kDa) nonchromophoric NOM can adsorb to internal adsorption sites in carbon particles. Therefore, SPAC and PAC adsorb low-MW NOM to a similar extent.

NOM that competes with geosmin for adsorption is a very-low-MW (<230 Da) chromophoric NOM, as is the NOM that competes with another micro-pollutant, MIB. The NOM fraction that competes with a target compound for adsorption has a molecular weight similar to that of the target compound. We estimate that the competing NOM accounts for <2% of the total DOC.

- The competing NOM can also adsorb onto internal adsorption sites in carbon particles. Although there is higher NOM loading onto SPAC than PAC, the NOM effect on micro-pollutant adsorption capacity is no more severe for SPAC than for PAC, because SPAC and PAC adsorb the competing NOM, which accounts for only a small fraction of the entire NOM, to a similar extent

Acknowledgements

This study was supported by Grant-in-Aid for Scientific Research A(21246083), S(24226012) and Challenging Exploratory Research (23656323) from the Japan Society for the Promotion of Science, by Health and Labour Sciences Research Grant (Research on Health Security Control) of Japan, and by Metawater Co., Tokyo, Japan.

Appendix A. Supplementary material

Supplementary data associated with this article can be found, in the online version, at http://dx.doi.org/10.1016/j.seppur.2013.04.009.

References

[1] W.F. Young, H. Horth, R. Crane, T. Ogden, M. Arnott, Taste and odour threshold concentrations of potential potable water contaminants, Water Res. 30 (2) (1996) 331–340.
[2] J.L. Worley, A.M. Dietrich, R.C. Hoehn, Dechlorination techniques to improve sensory odor testing of geosmin and 2-MIB, J. Am. Water Works Assoc. 95 (3) (2003) 109–117.
[3] R. Srinivasan, G.A. Sorial, Treatment of taste and odor causing compounds 2-methyl isoborneol and geosmin in drinking water: a critical review, J. Environ. Sci. 23 (1) (2011) 1–13.
[4] H. Sontheimer, J.C. Crittenden, R.S. Summers, Activated Carbon for Water Treatment, second ed., DVGW-Forschungsstelle, Karlsruhe, Germany, 1988.
[5] Y. Matsui, Y. Fukuda, R. Murase, N. Aoki, S. Mima, T. Inoue, T. Matsushita, Micro-ground powdered activated carbon for effective removal of natural organic matter during water treatment, Water Sci. Technol.: Water Supply 4 (4) (2004) 155–163.
[6] Y. Matsui, R. Murase, T. Sanogawa, H. Aoki, S. Mima, T. Inoue, T. Matsushita, Rapid adsorption pretreatment with submicrometre powdered activated carbon particles before microfiltration, Water Sci. Technol. 51 (6–7) (2005) 249–256.
[7] Y. Matsui, T. Aizawa, F. Kanda, N. Nigorikawa, S. Mima, Y. Kawase, Adsorptive removal of geosmin by ceramic membrane filtration with super-powdered activated carbon, J. Water Supply Res. Technol.-AQUA 56 (6–7) (2007) 411–418.
[8] Y. Matsui, N. Ando, H. Sasaki, T. Matsushita, K. Ohno, Branched pore kinetic model analysis of geosmin adsorption on super-powdered activated carbon, Water Res. 43 (12) (2009) 3095–3103.
[9] N. Ando, Y. Matsui, R. Kurotobi, Y. Nakano, T. Matsushita, K. Ohno, Comparison of natural organic matter adsorption capacities of super-powdered activated carbon and powdered activated carbon, Water Res. 44 (14) (2010) 4127–4136.
[10] Y. Matsui, Y. Nakano, N. Ando, H. Sasaki, K. Ohno, T. Matsushita, Geosmin and 2-methylisoborneol adsorption on super-powdered activated carbon in the presence of natural organic matter, Water Sci. Technol. 62 (11) (2010) 2664–2668.
[11] Y. Matsui, T. Yoshida, S. Nakao, D.R.U. Knappe, T. Matsushita, Characteristics of competitive adsorption between 2-methylisoborneol and natural organic matter on superfine and conventionally sized powdered activated carbons, Water Res. 46 (15) (2012) 4741–4749.
[12] M.R. Graham, R.S. Summers, M.R. Simpson, B.W. MacLeod, Modeling equilibrium adsorption of 2-methylisoborneol and geosmin in natural waters, Water Res. 34 (8) (2000) 2291–2300.
[13] D.R.U. Knappe, Y. Matsui, V.L. Snoeyink, P. Roche, M.J. Prados, M.M. Bourbigot, Predicting the capacity of powdered activated carbon for trace organic compounds in natural waters, Environ. Sci. Technol. 32 (11) (1998) 1694–1698.
[14] S. Qi, L. Schideman, B.J. Mariñas, V.L. Snoeyink, C. Campos, Simplification of the IAST for activated carbon adsorption of trace organic compounds from natural water, Water Res. 41 (2) (2007) 440–448.
[15] G. Newcombe, J. Morrison, C. Hepplewhite, D.R.U. Knappe, Simultaneous adsorption of MIB and NOM onto activated carbon – II. competitive effects, Carbon 40 (12) (2002) 2147–2156.
[16] International Humic Substance Society, <http://www.ihss.gatech.edu/soilhafa.html>, (accessed 23.04.12).
[17] Y. Matsui, N. Ando, T. Yoshida, R. Kurotobi, T. Matsushita, K. Ohno, Modeling high adsorption capacity and kinetics of organic macromolecules on super-powdered activated carbon, Water Res. 45 (4) (2011) 1720–1728.
[18] H.J. Motulsky, A. Christopoulos, Fitting Models to Biological Data Using Linear and Nonlinear Regression: A Practical Guide to Curve Fitting, Oxford University Press, New York, 2004.

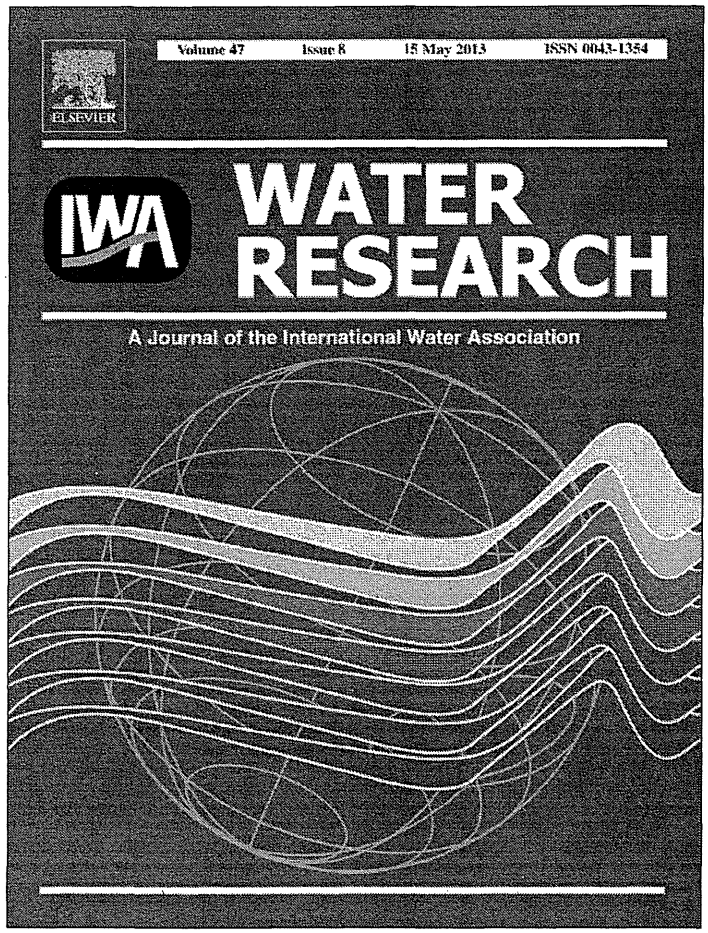

WATER RESEARCH 47 (2013) 2873–2880

Available online at www.sciencedirect.com

SciVerse ScienceDirect

journal homepage: www.elsevier.com/locate/watres

Geosmin and 2-methylisoborneol removal using superfine powdered activated carbon: Shell adsorption and branched-pore kinetic model analysis and optimal particle size

Yoshihiko Matsui [a,*], Soichi Nakao [b], Takuma Taniguchi [b], Taku Matsushita [a]

[a] Faculty of Engineering, Hokkaido University, N13W8, Sapporo 060-8628, Japan
[b] Graduate School of Engineering, Hokkaido University, N13W8, Sapporo 060-8628, Japan

ARTICLE INFO

Article history:
Received 19 July 2012
Received in revised form
18 February 2013
Accepted 23 February 2013
Available online 13 March 2013

Keywords:
Taste and odor
Water treatment
PAC
SPAC
Contact time

ABSTRACT

2-Methylisoborneol (MIB) and geosmin are naturally occurring compounds responsible for musty-earthy taste and odor in public drinking-water supplies, a severe problem faced by many utilities throughout the world. In this study, we investigated adsorptive removal of these compounds by superfine powdered activation carbon (SPAC, particle size <1 μm) produced by novel micro-grinding of powdered activated carbon; we also discuss the optimization of carbon particle size to efficiently enhance the adsorptive removal. After grinding, the absorptive capacity remained unchanged for a 2007 carbon sample and was increased for a 2010 carbon sample; the capacity increase was quantitatively described by the shell adsorption model, in which MIB and geosmin adsorbed more in the exterior of a carbon particle than in the center. The extremely high uptake rates of MIB and geosmin by SPAC were simulated well by a combination of the branched-pore kinetic model and the shell adsorption model, in which intraparticle diffusion through macropores was followed by diffusion from macropore to micropore. Simulations suggested that D_{40} was on the whole the best characteristic diameter to represent a size-disperse group of adsorbent particles; D_{40} is the diameter through which 40% of the particles by volume pass. Therefore, D_{40} can be used as an index for evaluating the improvement of adsorptive removal that resulted from pulverization. The dose required for a certain percentage removal of MIB or geosmin decreased linearly with carbon particle size (D_{40}), but the dose reduction became less effective as the activated carbon was ground down to smaller sizes around a critical value of D_{40}. For a 60-min contact time, critical D_{40} was 2–2.5 μm for MIB and 0.4–0.5 μm for geosmin. The smaller critical D_{40} was when the shorter the carbon–water contact time was or the slower the intraparticle mass transfer rate of an adsorbate was.

1. Introduction

For drinking water suppliers, removing any objectionable tastes and odors is key to ensuring customer satisfaction. Two important compounds, geosmin and 2-methylisoborneol (MIB), impart a strong musty-earthy taste and odor that lead to customer complaints even at concentrations as low as 10 ng/L. These compounds are the metabolites of various microorganisms, including cyanobacteria. Japan's drinking water quality standard regulates geosmin and MIB concentrations in tap water to be lower than 10 ng/L each; this is the lowest concentration level among other constituents. Effective and accepted treatment options to control taste and odor compounds include ozone oxidation and adsorption using

* *Corresponding author.* Tel./fax: +81 11 706 7280.
E-mail address: matsui@eng.hokudai.ac.jp (Y. Matsui).
0043-1354/$ – see front matter © 2013 Elsevier Ltd. All rights reserved.
http://dx.doi.org/10.1016/j.watres.2013.02.046

granular or powdered activated carbon (PAC). Among these options, PAC treatment is the simplest method and perhaps the most widely applied (e.g., Srinivasan and Sorial, 2011), but is rather expensive compared to conventional treatment processes such as coagulation treatment, in particular when it is used on a continuous basis. A key difficulty with PAC is that the adsorption of MIB and geosmin is relatively slow. A very long PAC–water contact time is essential to utilize the PAC's full adsorptive capacity (Huang et al., 1996; Gillogly et al., 1998; Cook et al., 2001); alternatively, a higher dose of PAC can be used, but this increases treatment cost.

PAC's effectiveness as an adsorbent is influenced by various characteristics, including its surface chemistry, pore structure, and particle size. Micropore volume and oxygen content are key properties affecting the equilibrium adsorption capacity of activated carbon (Pendleton et al., 1997; Considine et al., 2001; Nowack et al., 2004; Yu et al., 2007; Tennant and Mazyck, 2007). Besides equilibrium capacity, adsorption kinetics is another important aspect of adsorptive removal, and smaller adsorbent particles have faster adsorption kinetics (e.g., Najm et al., 1990). Accordingly, reducing particle size to improve PAC's adsorbate uptake rate is one measure to more efficiently utilize its adsorptive capacity. Although adsorption kinetics can be enhanced by reducing the activated carbon particle size, the overall adsorption capacity is unaffected by particle size because adsorption occurs in the internal pores of the activated carbon particles (Letterman et al., 1974; Peel and Benedek, 1980; Leenheer, 2007). However, the recent advent of superfine powdered activated carbon (SPAC) has renewed discussions on the relationship between particle size and adsorption capacity as well as it has prompted new discussions on the relationship in the sub-micron domain (Matsui et al., 2004, 2005; Heijman et al., 2009). Smaller activated carbon particles have been reported to have greater adsorption capacity for some macromolecules, including natural organic matter (NOM); the dependency of adsorption capacity on adsorbent size is well described by the shell adsorption model (SAM; Ando et al., 2010; Matsui et al., 2011). SPAC is also superior to PAC in removing geosmin and mitigating membrane fouling when it is used in adsorption pretreatment before microfiltration (Matsui et al., 2007, 2009b; Huang et al., 2009).

The homogeneous surface diffusion model (HSDM) has traditionally been used to predict the effect of adsorbent particle size on kinetics (Huang et al., 1996; Cook et al., 2001; Newcombe and Cook, 2002). However, HSDM does not accurately describe geosmin adsorption on adsorbents of different particle sizes, such as SPAC and PAC, unless the model is modified to vary surface diffusivity according to changes in carbon particle size (Matsui et al., 2009a). Therefore, HSDM does not truly predict the effect of carbon particle size on adsorptive removal. The branched-pore kinetic model (BPKM), which consists of macropore diffusion followed by mass transfer from macropore to micropore, accurately describes the adsorption kinetics on SPAC and PAC with the same set of model parameter values, including surface diffusivity. In a previous study (Matsui et al., 2009a), BPKM was used in conjunction with the Freundlich isotherm equation, and the adsorption isotherms of SPAC and PAC were assumed to be the same. However, the use of BPKM to model adsorption kinetics on the assumption that the adsorption capacities of SPAC and PAC are different has not been tested. Moreover, BPKM has not been applied to the removal of MIB or MIB/geosmin in natural water systems. The relationship between MIB and geosmin removal rates and adsorbent particle size has not yet been fully analyzed, particularly in the micron and submicron range.

In the present study, we performed adsorption equilibrium and kinetics experiments to assess the capacity and the rate of MIB and geosmin uptake onto SPAC and PAC, both in the presence of NOM and in single-solute systems. To consider the effects of carbon particle size on both adsorption capacity and kinetics, we applied BPKM in conjunction with SAM. In this paper we discuss the effects of activated carbon particle size, as well as optimum particle size.

2. Materials and methods

2.1. *Activated carbon*

Commercially available wood-based PAC (Taikou-W, Futamura Chemical Industries Co., Gifu, Japan) was obtained in the years 2007 and 2010. SPAC was prepared by pulverizing PAC in a wet bead mill (Metawater Co., Tokyo, Japan). Both PAC and SPAC samples were slurried in ultrapure water and were stored at 4 °C. In this paper, we refer to the as-received PAC obtained in 2007 as PAC07 and that obtained in 2010 as PAC10. The pulverized carbons are referred to similarly as SPAC07 and SPAC10. We also prepared another set of pulverized carbons with median diameters between those of PAC and SPAC; these are referred to as SPACb07 and SPACb10. Particle size distributions of the activated carbon samples were determined using a laser-light scattering instrument (LA-700, Horiba, Kyoto, Japan); the samples were prepared for analysis by suspension of SPAC/PAC in water to make 200-mL samples containing 0.001–0.01% carbon, followed by addition of a dispersant (0.02 mL of an 18% solution of anionic surfactant) and ultrasonication for 4 min Table 1 summarizes the properties of each activated carbon.

2.2. *Water samples*

Water containing NOM was collected from Lake Hakucho, Hokkaido, Japan. The sample was transported in polyethylene tanks and stored at 4 °C. The water was filtered through a 0.2-μm-pore membrane (DISMIC-25HP; Toyo Roshi Kaisha, Tokyo) and diluted to adjust the dissolved organic carbon concentration to ~1.5 mg/L; the diluent used for this purpose was prepared by amending ultrapure water (Milli-Q Advantage, Millipore Co.) with salts to obtain an ionic composition similar to that used in a previous study (Matsui et al., 2012). Stock solutions of MIB and geosmin were prepared by dissolving the pure chemicals (Wako Pure Chemical Industries, Osaka, Japan) in ultrapure water. The dissolution was confirmed by 0.2-μm membrane filtering. The NOM-containing waters (NOMWs) were spiked with the MIB or geosmin stock solutions to prepare samples with an initial MIB or geosmin concentration of ~1 μg/L. For single-solute MIB and geosmin experiments, the MIB or geosmin stock solution was added to ultrapure water amended with inorganic ions such that the ionic composition was similar to that of the NOMW; we refer to this water as organic-free water (OFW). All water samples were filtered

Table 1 – Size and surface area characteristics of the activated carbon particles studied.

Sample name	Median diameter (D_{50}, μm)	Effective diameter (D_{10}, μm)	Uniformity coefficient	Geometric standard deviation	BET surface area (m^2/g)
PAC07	11.8	3.89	3.27	2.27	1170
SPACb07	1.91	0.904	2.34	1.85	n/a
SPAC07	0.725	0.271	3.15	1.93	1110
PAC10	13.5	3.35	5.19	2.80	1070
SPACb10	4.87	0.853	7.59	3.29	n/a
SPAC10	0.857	0.396	2.70	3.00	1130

through a 0.2-μm-pore membrane before use. MIB and geosmin concentrations were analyzed using a purge-and-trap concentrator coupled to a gas chromatograph equipped with a mass spectrometer (GCMS-QP2010 Plus; Shimadzu Corp., Kyoto, Japan; Aqua PT 5000 J, GL Sciences Inc., Tokyo, Japan). Dissolved organic carbon was quantified using a Model 810 carbon analyzer (Sievers Instruments, Inc., Boulder, CO, USA).

2.3. Batch adsorption tests

In adsorption equilibrium tests, 150-mL aliquots of OFW or NOMW spiked with MIB or geosmin ($C_0 = \sim 1$ μg/L) were transferred to 160-mL vials. A specified amount of SPAC/PAC was immediately added, the vials were manually shaken, and then the samples were agitated on a mechanical shaker for one week at a constant temperature of 20 °C. In a preliminary experiment, it was confirmed that MIB and geosmin adsorption equilibriums were reached within one week and that NOM adsorption nearly reached equilibrium. Several bottles that did not contain PAC or SPAC were used as control samples to confirm that the concentrations of MIB, geosmin, and NOM changed negligibly during long-term agitation. After water samples were filtered through a 0.2-μm-pore membrane filter, the MIB and geosmin concentrations in the aqueous phase were measured. Solid-phase concentrations of each adsorbate were calculated from the mass that remained in the aqueous phase.

Adsorption kinetics was investigated with sample waters (3 L or 1 L) each containing MIB or geosmin ($C_0 = \sim 1$ μg/L) in a beaker with efficient mixing (200 rpm). After the addition of a specified amount of activated carbon suspension, aliquots were withdrawn at intervals and filtered immediately through a 0.2-μm-pore membrane filter for analysis of the aqueous MIB and geosmin concentrations.

3. Results and discussion

3.1. Equilibrium and kinetics of adsorption

Adsorption equilibrium tests were conducted for MIB and geosmin in the OFW system to compare SPAC with PAC. SPAC07 and SPACb07 had slightly greater MIB adsorption capacity than PAC07, but the difference (11%) was very small (Fig. 1A). This result suggests that grinding did not effectively increase the MIB adsorption capacity of PAC07. SPAC10 and

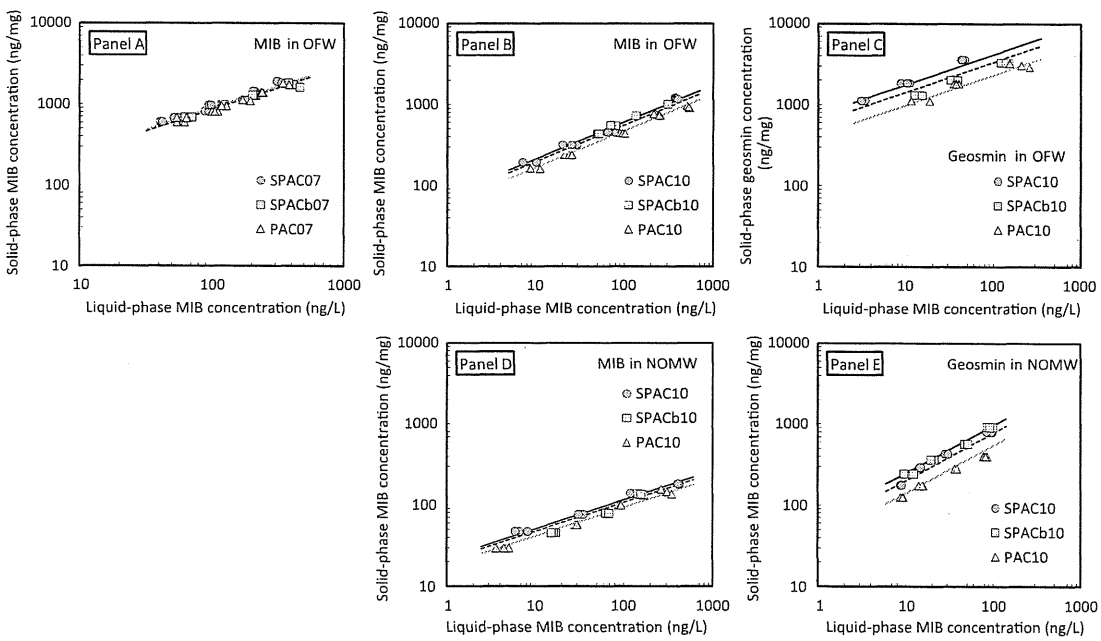

Fig. 1 – Adsorption isotherms for MIB (Panels A, B, and D) and geosmin (Panels C and E). Experimental data are shown as points, and SAM fits to the data are shown as lines. The SAM fit parameters are as follows: Panel A–K_0: 3.1 (mg/g)/(ng/L)$^{1/n}$, δ: 38.6, 1/n: 0.54. Panel B–K_0: 1.8 (mg/g)/(ng/L)$^{1/n}$, δ: 9.1, 1/n: 0.46. Panel C–K_0: 10.7 (mg/g)/(ng/L)$^{1/n}$, δ: 3.0, 1/n: 0.37. Panel D–K_0: 0.3 (mg/g)/(ng/L)$^{1/n}$, δ: 11.0, 1/n: 0.36. Panel E–K_0: 4.1 (mg/g)/(ng/L)$^{1/n}$, δ: 3.2, 1/n: 0.59.

SPACb10 showed a somewhat greater increase in MIB adsorption capacity relative to that of PAC10; the capacity of SPAC10 was 27% greater than that of PAC10 (Fig. 1B). For geosmin, the adsorption capacity difference was more pronounced, with the clear trend SPAC10 > SPACb10 > PAC10 (Fig. 1C). We also conducted adsorption equilibrium tests by using natural water spiked with MIB or geosmin to elucidate the superiority of SPAC over PAC for removing MIB and geosmin under the influence of NOM. Adsorption isotherms of MIB in the presence of NOM show that SPAC10 had 23% more MIB adsorption capacity than PAC10 under this condition. The presence of NOM reduced the MIB adsorption capacity on SPAC by 85% while it reduced the capacity on PAC by 84% indicating that the adsorption capacities of SPAC and PAC were reduced to a similar extent by competitive adsorption of NOM (Fig. 1D). The same influence of NOM on the adsorption capacity between SPAC and PAC suggests the same loading of NOM that compete with MIB for adsorption sites. Details for the effect of NOM loading on SPAC and PAC adsorption are seen elsewhere (Matsui et al., 2012). The presence of NOM also reduced the geosmin adsorption capacities of SPAC and PAC to a similar extent (Fig. 1E); as with MIB, the geosmin adsorption capacity of SPAC10 in the presence of NOM was also higher than that of PAC10.

The phenomenon that grinding carbon particles to reduce their size increased adsorption capacity is explained by means of a mechanism whereby molecules do not completely penetrate the adsorbent particle and instead preferentially adsorb near the outer surface of the particle (Ando et al., 2010), and the observed changes in adsorption isotherms according to carbon particle size are described well by SAM (see lines in Fig. 1; see also Matsui et al., 2011), which was originally developed to describe the adsorption of NOM. In SAM, the adsorption capacity parameter, that is, the Freundlich K value, decreases linearly with distance from the external surface to a certain depth:

$$K_S(r,R) = K_0 \left[\max\left(\frac{r-R+\delta}{\delta}, 0\right)\right] \quad (1)$$

where r is the radial distance from the center of an adsorbent particle (cm), R is the adsorbent particle radius (cm); $K_S(r, R)$ is the Freundlich adsorption capacity parameter ((ng/mg)/(ng/L)$^{1/n}$), which varies as a function of radial distance r and adsorbent radius R; K_0 is the Freundlich parameter of adsorption at the external adsorbent particle surface ((ng/mg)/(ng/L)$^{1/n}$); δ is the penetration depth, or in other words the thickness of the penetration shell (cm); and n is the dimensionless Freundlich exponent.

In contrast to the adsorption equilibria, the adsorption kinetics of SPAC and PAC were extremely different: SPAC had a much faster uptake rate than PAC under every condition studied (Fig. 2). In both OFW and NOMW systems, uptake rates of geosmin and MIB were improved greatly by using SPAC. For example, a 0.5 mg/L dose of SPAC removed geosmin at almost the same rate as 3 mg/L of PAC (Fig. 2C). PAC would show little removal if the dosage was 0.5 mg/L, that was the same as that of SPAC, but this experiment was not conducted because the objective of the experiments was model parameter determination, where the data of little removal was ineffective.

These experimental data of adsorption kinetics were simulated by applying BPKM (Matsui et al., 2009a), modified by incorporating SAM to describe the local adsorption equilibria in internal pores of the carbon particle. The original BPKM assumes radial intraparticle diffusion through macropores in an adsorbed state (surface diffusion). However, the surface diffusion scenario could not be applied in this study, because it assumes that the interior of the activated carbon particle is homogeneous. Such homogeneity implies that adsorbed

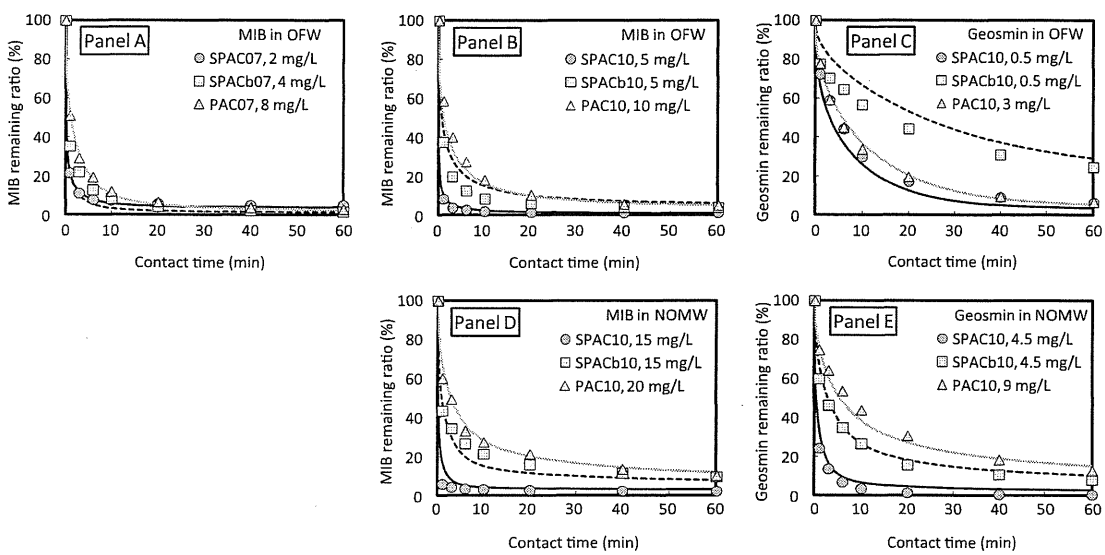

Fig. 2 – Adsorption kinetics for MIB (Panels A, B, and D) and geosmin (Panels C and E). Experimental data are shown as points, and BPKM-SAM simulations are shown as lines. Initial MIB and geosmin concentrations are ~1 μg/L. The BPKM-SAM parameters are as follows: Panel A – D_P: 1.7 × 10^{-7} cm^2/s, K_S: 8.7 × 10^{-4} s^{-1}, ϕ: 0.57. Panel B – D_P: 3.1 × 10^{-7} cm^2/s, K_S: 3.9 × 10^{-4} s^{-1}, ϕ: 0.73. Panel C – D_P: 2.1 × 10^{-7} cm^2/s, K_S: 3.8 × 10^{-4} s^{-1}, ϕ: 0.29. Panel D – D_P: 3.0 × 10^{-7} cm^2/s, K_S: 2.1 × 10^{-3} s^{-1}, ϕ: 0.55. Panel E – D_P: 0.44 × 10^{-7} cm^2/s, K_S: 1.5 × 10^{-3} s^{-1}, ϕ: 0.53.

molecules have migrated into adsorbent particles by Fick's first law of diffusion according to a local solid-phase concentration gradient, and that adsorbate molecules are ultimately distributed evenly across the inside surface of an adsorbent such that local solid-phase concentrations become equal. Such a scenario is inconsistent with SAM. Therefore, instead of modeling diffusion in an adsorbed state, we modeled diffusion of molecules in liquid-filled macropores (pore diffusion). Mass transfer resistance across the liquid film external to adsorbent particle surfaces was substantially neglected by giving a large value (10 cm/s) of liquid film mass transfer coefficient because it cannot be the rate-determining step in well mixed reactors (Sontheimer et al., 1988; Matsui et al., 2009a).

Finally, the macropore mass balance equation is as follows:

$$\phi\frac{\partial q_M(t,r,R)}{\partial t}=\frac{\varnothing D_P}{\rho r^2}\frac{\partial}{\partial r}\left(r^2\frac{\partial c_M(t,r,R)}{\partial r}\right)-k_B\left[q_M(t,r,R)-q_B(t,r,R)\right] \quad (2)$$

where t is adsorption time in the batch system (s); ϕ is the fraction of adsorptive capacity available in the macropore region (dimensionless); ρ is the adsorbent particle's density (g/L); D_P is the diffusion coefficient in the macropore (cm^2/s); c_M (t, r, R) is the liquid-phase concentration in a macropore of an adsorbent of radius R, at radial distance r and time t (ng/L); q_M (t, r, R) is the solid-phase concentration in a macropore of an adsorbent of radius R, at radial distance r and time t (ng/g); q_B (t, r, R) is the solid-phase concentration in a micropore of an adsorbent of radius R, at radial distance r and time t (ng/g); and k_B is the rate coefficient for mass transfer between macropores and micropores (s^{-1}).

The local adsorption equilibrium is expressed as follows:

$$c_M(t,r,R)=\left(\frac{q_M(t,r,R)}{K_S(r,R)}\right)^n \quad (3)$$

The other BPKM equations can be seen elsewhere (Matsui et al., 2009a).

Model simulations of both MIB and geosmin concentrations were overall successful in describing the curves of concentration vs. contact time in a batch adsorption system (see the lines in Fig. 2). Therefore, once the adsorption equilibrium and kinetic model parameters are determined, one can predict the MIB and geosmin concentrations at a given carbon–water contact time and a given carbon particle size distribution. Using this model, one can evaluate the effect of carbon particle size on the concentrations of MIB and geosmin remaining after a given contact time.

3.2. *Representative diameter for adsorption kinetics*

With the successful application of BPKM-SAM to MIB and geosmin adsorption in OFW and NOMW systems, it becomes possible to quantitatively evaluate the optimum adsorbent diameters for MIB and geosmin removal. A complicating factor in studying adsorption is that activated carbon products typically consist of particles with a wide size distribution, and the dispersity of this distribution also varies considerably among different products and preparations. Therefore, we first investigated a characteristic particle size that would best represent the entire size distribution of any given carbon sample. If a suitable definition of characteristic size can be found, this greatly simplifies the problem and allows us to understand the group's adsorption kinetics using a single size value (Traegner et al., 1996). Such a characteristic size should be a measure of central tendency, which is unaffected by the relatively few extreme values in the tails of the distribution. We tested several definitions of characteristic size: D_{20} (i.e., the diameter that 20% by volume of the all particles are finer than), D_{30}, D_{40}, D_{50}, and D_{60}. In selecting the best characteristic size, we created three fictitious particle size distributions (see Fig. 3): a uniform distribution (uniformity coefficient of 1.0), a moderate distribution with a uniformity coefficient of 2.34 (the value was taken from the actual particle size distribution of SPACb07), and a wider size distribution with a uniformity coefficient of 7.59 (the value was taken from SPACb10).

Using BPKM-SAM, we simulated geosmin concentration decay for the three adsorbents each having different particle size distributions but all having the same characteristic size. In the case of D_{40}, the three curves were not so different (Fig. 4), suggesting that the geosmin adsorption kinetics were almost the same among carbon samples whose D_{40} was the same, regardless of whether their particle size distribution was narrow or wide. The root mean square (RMS) of C/C_0 (remaining ratio) deviations between the moderate distribution with uniformity coefficient 2.34 and the wide distribution with 7.59 was 0.013, and the RMS value between the moderate distribution with 2.34 and the uniform distribution with 1.0 was 0.024. We conducted this kind of BPKM simulation for D_{20}, D_{30}, D_{40}, D_{50}, and D_{60}, for both MIB and geosmin and in both OFW and NOMW; for MIB removal, RMS was minimized using D_{40}, whereas D_{30} was optimal for geosmin (Fig. 5). Therefore, D_{40} was the best characteristic size to represent the kinetics of MIB removal (Fig. 5A), whereas D_{30} was the best for geosmin removal (Fig. 5B). We understand that for an adsorbate having a slow intraparticle mass transfer rate in a carbon particle, carbon fractions with small sizes, because they have relatively large external surface area, make a major contribution to adsorptive removal when contact times are limited. In such a

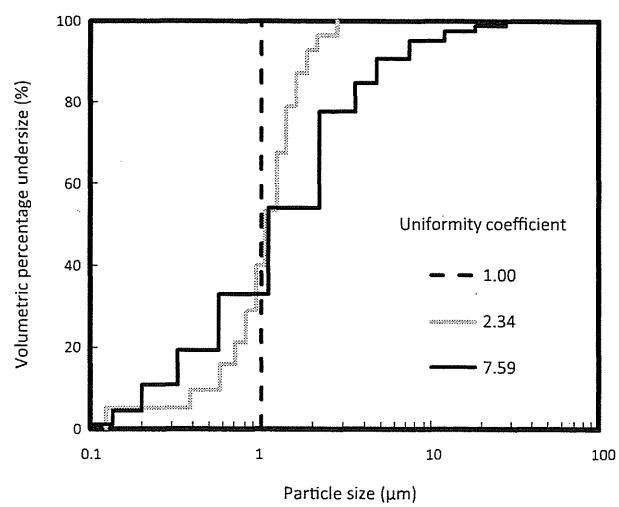

Fig. 3 – Fictitious adsorbent particle size distributions with the same D_{40} (1.0 μm) for BPKM-SAM simulations.

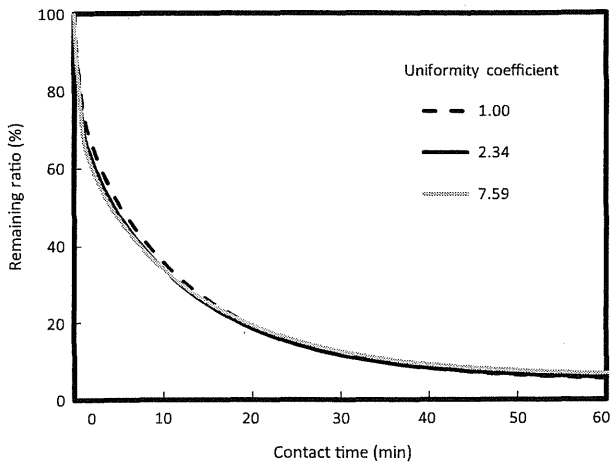

Fig. 4 – Effect of particle size distribution on adsorption kinetics of geosmin: BKAM-SAM simulations (D_{40} = 1.0 μm, activated carbon dose = 0.5 mg/L, initial geosmin concentration: 1000 ng/L, NOM water, D_S: 2.1×10^{-7} cm²/s, K_S: 3.8×10^{-4} s^{-1}, ϕ: 0.29).

case, one would expect that the most representative characteristic diameter would be less than the median diameter D_{50}. Because geosmin has a slower intraparticle mass transfer rate than MIB (as is indicated by the different curvatures of the concentration decay curves in Fig. 2 and by the comparison of the D_P and K_S values between Panels B and C and between Panels D and E for the same carbons in the figure caption), it is reasonable that the most representative diameter for geosmin removal (D_{30}) was more heavily weighted to the smaller size fraction than that of MIB (D_{40}). There was no single best representative size to describe the adsorption kinetics, but the RMS values of D_{30} and D_{40} were not so different. Overall, D_{40} was the best, as it minimized the total RMS (Fig. 5C). This representative diameter is expected to characterize adsorption kinetics well regardless of whether the size distribution is wide or narrow. Variations in size dispersity might result from variations in the type of grinder used, or the grinding time, but then this diameter could be used as an index to show whether the size was sufficiently small after grinding. In the present BPKM-SAM simulations, the particle size distribution of the adsorbent was taken into consideration, but most other research and practical applications of adsorption kinetics models assume uniform particle size to simplify calculations. We propose that D_{40} be used as a representative particle diameter in model simulations when a uniform particle size is assumed.

3.3. *Optimum diameter for efficient absorption*

The relationship between D_{40} and required dose was calculated through BPKM-SAM simulations. For a given contact time, the carbon dose required to effect a given removal percentage could be reduced by decreasing D_{40} (Fig. 6). Between D_{40} values of 5 and 50 μm, the relationship was roughly linear; for example, the required dose was reduced by one fifth when D_{40} was decreased by one fifth. Matsui et al. (2007) compared the SPAC and PAC doses required for 60–98% geosmin removal in a system using flow-through PAC adsorption followed by microfiltration separation, and reported that the SPAC (D_{50} = 0.65 μm) dose required for a 4-min PAC–water contact time was 6–25% that of the PAC (D_{50} = 7.6 μm) dose for the same removal and contact time. In our analysis of geosmin removal, the corresponding dose ratio was 10% for a 90% removal (10% remaining ratio) over a 10-min contact time (Fig. 6C and E). Although removal efficiencies may differ between flow-through and batch reactors, the results of the current study are generally consistent with the previous study.

In the scenarios modeled, the required dose initially decreased linearly with the particle size, but this trend leveled off as D_{40} reached a critical range (Fig. 6). That is to say, for a given contact time and removal ratio, reducing the particle size to a certain degree effectively reduced the required carbon dose, but eventually further size reduction was not worthwhile. It is convenient to define a critical D_{40} value below which further grinding was not useful; we define critical D_{40} at the intersection between the line extrapolated from the linear dose decline and the constant line representing the lowest dose (for an example, see Fig. 6A). As shown in Fig. 7, critical D_{40} was larger for longer contact times, reflecting the fact that adsorption capacity becomes progressively more important than kinetics as contact time is increased. The critical D_{40} value for MIB removal was ~1 μm for a 10-min contact time, but the values were 2–2.5 and 3–4 μm for contact times of 60 and 180 min, respectively; critical D_{40} values for geosmin removal were ~0.2, 0.4–0.5, and 0.5–0.8 μm for contact times of 10, 60, and 180 min, respectively. As just mentioned, adsorption capacity becomes relatively more important than kinetics as contact time increases. When contact times are long, only the large particles will fail to reach adsorption equilibrium, so only these large particles will have

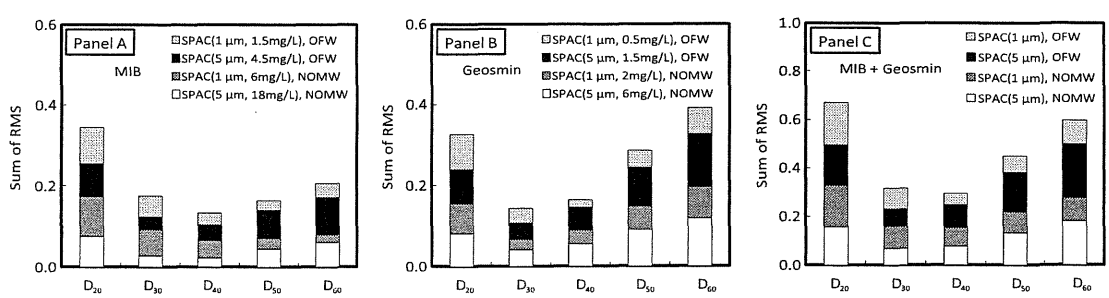

Fig. 5 – Sums of root mean square (RMS) values to select the best characteristic size that represents a group of adsorbent particles with the same size distribution (Initial MIB or geosmin concentration is 1000 ng/L).

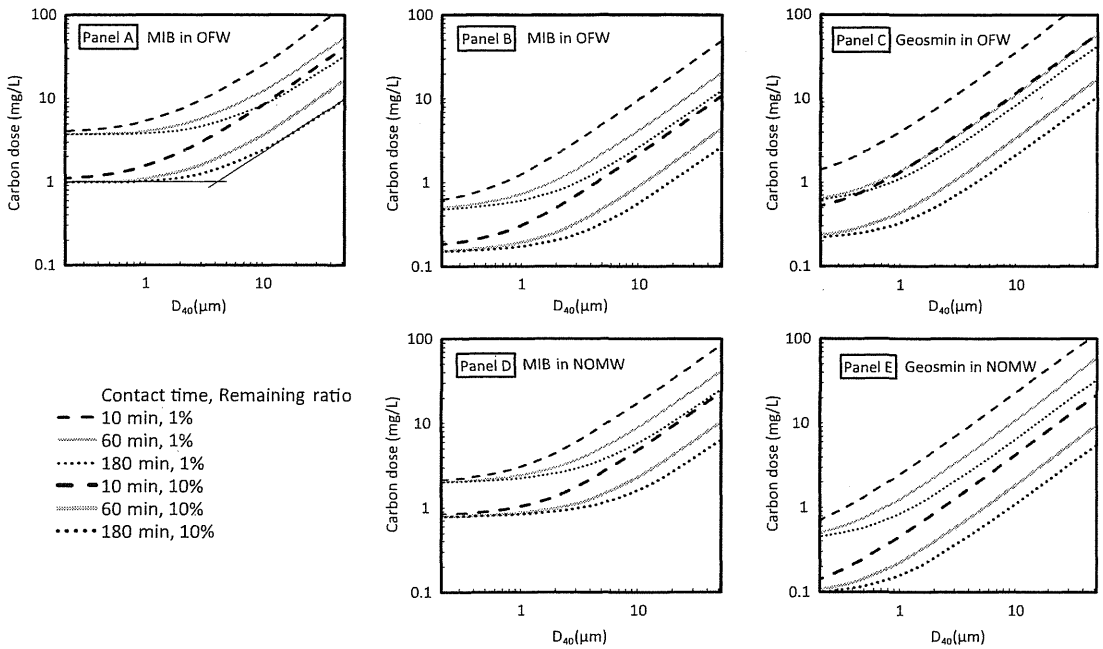

Fig. 6 – Dose required for various removal percentages and contact times vs. particle size of activated carbon for MIB (Panels A, B, and D) and geosmin (Panels D and E) removal: PBKM-SAM simulations. Initial concentration is 1000 ng/L. PBKM-SAM parameter values are the same as those of Figs. 1 and 2. Panel A: Carbon sample from the year 2007. Panels B–E: Carbon sample from the year 2010.

any potential for improvement of kinetics through particle size reduction. For these large particles, therefore, adsorption kinetics does still play a role even for longer contact times. Importance of adsorption kinetics only for large particles means that the critical D_{40} increases for longer contact times.

Critical D_{40} was smaller for geosmin than for MIB. As stated earlier, geosmin has slower intraparticle mass transfer within a carbon particle, meaning that adsorption kinetics plays a more important role in determining the necessary dose. Accordingly, within a size range below the critical D_{40} for MIB removal, continued reduction in size was irrelevant to MIB removal but continued to reduce the necessary dose for the equivalent geosmin removal. Using small adsorbent particles brought about fast adsorptive removal, but this effect became less important as contact time was increased. Overall, grinding activated carbon until its representative diameter D_{40} was a few microns was found to be an effective method for enhancing its adsorptivity and thereby enabling a reduction in its dose.

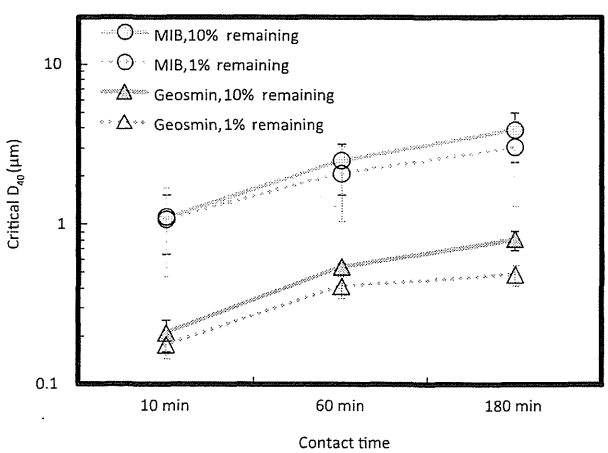

Fig. 7 – Effect of carbon–water contact time on the critical D_{40} value.

4. Conclusions

1. Owing to decreased carbon particle size, removal of MIB and geosmin over a given contact time was greatly enhanced. The change in adsorption isotherms with decreased particle size was explained by SAM. Irrespective of the adsorbent particle size, adsorption kinetics was well simulated by BPKM combined with SAM, using a given set of model parameter values.
2. BPKM-SAM simulations suggested that D_{40}, the diameter that 40% by volume of all the particles are finer than, was a suitable characteristic diameter that represented the adsorption kinetics of adsorbent particles well regardless of their size dispersity. Therefore, if a model simulation is simplified by assuming uniform adsorbent particle size, we propose that D_{40} be used as the representative diameter.
3. The activated carbon dose required to effect a certain removal percentage was reduced in proportion to carbon particle size represented by D_{40}, but this effect leveled off as D_{40} fell below a certain size. This critical D_{40} value depended on the carbon–water contact time and the intraparticle mass transfer rate of adsorbate in a carbon particle; these

factors determine the relative importance of adsorption capacity and kinetics on adsorptive removal.

4. Because of the kinetics enhancements that smaller particles provide, the merit of reducing particle size through grinding continued into a smaller size domain for systems that used shorter carbon–water contact times. Similarly, because geosmin was adsorbed more slowly than MIB, further reductions in particle size beyond MIB's leveling-off point continued to have greater merit for geosmin removal. The critical D_{40} values of MIB were ~1 and 3–4 μm for 10- and 180-min contact times, respectively, whereas those of geosmin were ~0.2 and 0.5–0.8 μm, respectively. Overall, grinding activated carbon until its representative diameter D_{40} was a few microns improved the speed of MIB and geosmin removal and/or reduced the needed dose over a wide range of conditions.

Acknowledgments

This study was supported by Grant-in-Aid for Scientific Research A (21246083) and S (24226012) from the Japan Society for the Promotion of Science; by Health and Labour Sciences Research Grant (Research on Health Security Control) of Japan; and by Metawater Co., Tokyo, Japan.

REFERENCES

Ando, N., Matsui, Y., Kurotobi, R., Nakano, Y., Matsushita, T., Ohno, K., 2010. Comparison of natural organic matter adsorption capacities of super-powdered activated carbon and powdered activated carbon. Water Research 44 (14), 4127–4136.

Considine, R., Denoyel, R., Pendleton, P., Schumann, R., Wong, S.-H., 2001. The influence of surface chemistry on activated carbon adsorption of 2-methylisoborneol from aqueous solution. Colloids and Surfaces A: Physicochemical and Engineering Aspects 179 (2), 271–280.

Cook, D., Newcombe, G., Sztajnbok, P., 2001. The application of powdered activated carbon for MIB and geosmin removal: predicting PAC doses in four raw waters. Water Research 35 (5), 1325–1333.

Gillogly, T.E.T., Snoeyink, V.L., Elarde, J.R., Wilson, C.M., Royal, E.P., 1998. ^{14}C-MIB adsorption on PAC in natural water. Journal of the American Water Works Association 90 (1), 98–108.

Heijman, S.G.J., Hamad, J.Z., Kennedy, M.D., Schippers, J., Amy, G., 2009. Submicron powdered activated carbon used as a pre-coat in ceramic micro-filtration. Desalination & Water Treatment 9, 86–91.

Huang, C., VanBenschoten, J.E., Jensen, J.N., 1996. Adsorption kinetics of MIB and geosmin. Journal of the American Water Works Association 88 (4), 116–128.

Huang, H., Schwab, K., Jacangelo, J.G., 2009. Pretreatment for low pressure membranes in water treatment: a review. Environmental Science & Technology 43 (9), 3011–3019.

Leenheer, J.A., 2007. Progression from model structures to molecular structures of natural organic matter components. Annals of Environmental Science 1, 57–68.

Letterman, R.D., Quon, J.E., Gemmell, R.S., 1974. Film transport coefficient in agitated suspensions of activated carbon. Journal of the Water Pollution Control Federation 46 (11), 2536–2547.

Matsui, Y., Fukuda, Y., Murase, R., Aoki, N., Mima, S., Inoue, T., Matsushita, T., 2004. Micro-ground powdered activated carbon for effective removal of natural organic matter during water treatment. Water Science and Technology: Water Supply 4 (4), 155–163.

Matsui, Y., Murase, R., Sanogawa, T., Aoki, N., Mima, S., Inoue, T., Matsushita, T., 2005. Rapid adsorption pretreatment with submicrometre powdered activated carbon particles before microfiltration. Water Science and Technology 51 (6–7), 249–256.

Matsui, Y., Aizawa, T., Kanda, F., Nigorikawa, N., Mima, S., Kawase, Y., 2007. Adsorptive removal of geosmin by ceramic membrane filtration with super-powdered activated carbon. Journal of Water Supply: Research and Technology-AQUA 56 (6–7), 411–418.

Matsui, Y., Ando, N., Sasaki, H., Matsushita, T., Ohno, K., 2009a. Branched pore kinetic model analysis of geosmin adsorption on super-powdered activated carbon. Water Research 43 (12), 3095–3103.

Matsui, Y., Hasegawa, H., Ohno, K., Matsushita, T., Mima, S., Kawase, Y., Aizawa, T., 2009b. Effects of super-powdered activated carbon pretreatment on coagulation and transmembrane pressure buildup during microfiltration. Water Research 43 (20), 5160–5170.

Matsui, Y., Ando, N., Yoshida, T., Kurotobi, R., Matsushita, T., Ohno, K., 2011. Modeling high adsorption capacity and kinetics of organic macromolecules on super-powdered activated carbon. Water Research 45 (4), 1720–1728.

Matsui, Y., Yoshida, T., Nakao, S., Knappe, D.R.U., Matsushita, T., 2012. Characteristics of competitive adsorption between 2-methylisoborneol and natural organic matter on superfine and conventionally sized powdered activated carbons. Water Research 46 (15), 4741–4749.

Najm, I., Snoeyink, V.L., Suidan, M.T., Lee, C.H., Richard, Y., 1990. Effect of particle size and background natural organics on the adsorption efficiency of PAC. Journal of the American Water Works Association 82 (1), 65–72.

Newcombe, G., Cook, D., 2002. Influences on the removal of tastes and odours by PAC. Journal of Water Supply Research and Technology-AQUA 51 (8), 463–474.

Nowack, K.O., Cannon, F.S., Mazyck, D.W., 2004. Enhancing activated carbon adsorption of 2-Methylisoborneol: methane and steam treatments. Environmental Science & Technology 38 (1), 276–284.

Peel, R.G., Benedek, A., 1980. Attainment of equilibrium in activated carbon isotherm studies. Environmental Science and Technology 14 (1), 66–71.

Pendleton, P., Wong, S.H., Schumann, R., Levay, G., Denoyel, R., Rouquero, J., 1997. Properties of activated carbon controlling 2-Methylisoborneol adsorption. Carbon 35 (8), 1141–1149.

Sontheimer, H., Crittenden, J.C., Summers, R.S., 1988. Activated Carbon for Water Treatment, second ed. DVGW-Forschungsstelle, Karlsruhe, Germany.

Srinivasan, R., Sorial, G.A., 2011. Treatment of taste and odor causing compounds 2-methyl isoborneol and geosmin in drinking water: a critical review. Journal of Environmental Sciences 23 (1), 1–13.

Tennant, M.F., Mazyck, D.W., 2007. The role of surface acidity and pore size distribution in the adsorption of 2-methylisoborneol via powdered activated carbon. Carbon 45 (4), 858–864.

Traegner, U.K., Suidan, M.K., Kim, B.R., 1996. Considering age and size distributions of activated-carbon particles in a completely-mixed adsorber at steady state. Water Research 30 (6), 1495–1501.

Yu, J., Yang, M., Lin, T.-F., Guo, Z., Zhang, Y., Gu, J., Zhang, S., 2007. Effects of surface characteristics of activated carbon on the adsorption of 2-methylisobornel (MIB) and geosmin from natural water. Separation and Purification Technology 56 (3), 363–370.